AGU PUBLICATIONS

Reviews of Geophysics

REVIEW ARTICLE
10.1002/2015RG000509

Key Points:
- Reviews the state of current knowledge of the low-frequency fluctuations of the extratropical troposphere
- Discusses the nonlinear regime paradigm and its effect on surface climate, and climate change
- Discusses the representation of nonlinear regimes in the state-of-the-art climate models

Correspondence to:
D. M. Straus,
dstraus@gmu.edu

Citation:
Hannachi, A., D. M. Straus, C. L. E. Franzke, S. Corti, and T. Woollings (2017), Low-frequency nonlinearity and regime behavior in the Northern Hemisphere extratropical atmosphere, *Rev. Geophys.*, *55*, 199–234, doi:10.1002/2015RG000509.

Received 22 OCT 2015
Accepted 25 JAN 2017
Accepted article online 28 JAN 2017
Published online 11 MAR 2017

Low-frequency nonlinearity and regime behavior in the Northern Hemisphere extratropical atmosphere

Abdel. Hannachi[1], David M. Straus[2], Christian L. E. Franzke[3], Susanna Corti[4], and Tim Woollings[5]

[1]Department of Meterology, MISU, Stockholm University, Stockholm, Sweden, [2]Center for Ocean-Land-Atmosphere Studies, George Mason University, Fairfax, Virginia, USA, [3]Meteorological Institute and Center for Earth System Research and Sustainability, University of Hamburg, Hamburg, Germany, [4]Institute of Atmospheric Sciences and Climate, National Research Council, Bologna, Italy, [5]Atmospheric, Oceanic and Planetary Physics, Department of Physics, Oxford University, Oxford, UK

Abstract The extratropical atmosphere is characterized by robust circulations which have time scales longer than that associated with developing baroclinic systems but shorter than a season. Such low-frequency variability is governed to a large extent by nonlinear dynamics and, hence, is chaotic. A useful aspect of this low-frequency circulation is that it can often be described by just a few quasi-stationary regime states, broadly defined as recurrent or persistent large-scale structures, that exert a significant impact on the probability of experiencing extreme surface weather conditions. We review a variety of techniques for identifying circulation regimes from reanalysis and numerical model output. While various techniques often yield similar regime circulation patterns, they offer different perspectives on the regimes. The regimes themselves are manifest in planetary scale patterns. They affect the structure of synoptic scale patterns. Extratropical flow regimes have been identified in simplified atmospheric models and comprehensive coupled climate models and in reanalysis data sets. It is an ongoing challenge to accurately model these regime states, and high horizontal resolutions are often needed to accurately reproduce them. The regime paradigm helps to understand the response to external forcing on a variety of time scales, has been helpful in categorizing a large number of weather types and their effect on local conditions, and is useful in downscaling. Despite their usefulness, there is a debate on the "nonequivocal" and systematic existence of these nonlinear circulation regimes. We review our current understanding of the nonlinear and regime paradigms and suggest future research.

1. Introduction

The atmosphere exhibits variations on a very wide range of space and time scales, from rapidly developing local weather systems, to jet streams which vary gradually throughout the season, to interannual variations of wintertime average temperature and precipitation, and to long-term decadal and centennial trends. The atmospheric circulation and thermodynamic evolution associated with all these scales are described by a set of highly nonlinear equations that must incorporate discontinuities due to the phase changes of water. Although weather is often defined by the complete state of the atmosphere at a particular instant, it is the most active circulation systems and the resultant extremes of precipitation, wind, and temperature that are of most interest. These active systems are generally associated with midlatitude cyclones, also called storms, which have highly baroclinic dynamics, spatial scales of several thousand kilometers, and time scales of several days. Climate, on the other hand, can be defined as the collection of long-term statistical properties of the system, as pointed out by *Lorenz* [1970]. A description of the climate would include not only the geographical distribution of temperature, rainfall, and winds but also the temporal variances and covariances which describe the typical locations of active storms, the so-called storm tracks. A link between the weather and climate can be seen already in the positive covariances between rapidly evolving meridional wind and temperature and moisture, which indicate the role of storms in maintaining the climate through consistent poleward transport of energy and water.

What may not be immediately apparent in the climate statistics of the atmosphere is the presence of extensive and robust intraseasonal variability, that is on time scales between roughly 10 and 50 days.

This "low-frequency" variability (hereafter LFV) encompasses changes in the background circulation (position of jets and zones of high baroclinicity) which cause significant modulation of the location and intensity of storms. A well-known example is the phenomenon of blocking, in which a strong high-pressure system steers the storms to its north or south for an extended period of time, causing spells of unusual weather in downstream locations. Another example is the slow movement of the maxima in zonal (eastward) winds or jets, which lead to changes in the location of the baroclinic zones.

The large-scale circulation described by LFV is often described in terms of weather regimes, which are characterized by recurrence and quasi-stationarity, also called persistence. It is these properties that are used to distinguish the LFV in a mathematical phase space, something that will be described later in this article. Note that in the tropics, intraseasonal LFV is dominated by the Madden-Julian Oscillation, which is a dominant slowly propagating mode of (ocean-atmosphere) coupled circulation and convective heating.

The existence of preferred intraseasonal large-scale flow structures in midlatitudes, also called circulation regimes, has been recognized since the early 1950s [*Rex*, 1950a, 1950b; *Namias*, 1950, 1964]. More recently, this field has attracted increasing interest because of the need to understand the predictable part of the atmosphere, such as low-frequency intraseasonal oscillations [*Branstator*, 1987] related to large-scale persistent flow patterns. Such patterns have been observed in the midlatitude atmosphere and have been noticed to persist for time periods much longer than those typical of midlatitude cyclones [*Namias*, 1950; *Horel*, 1985]. Put another way, the regime structures have time scales longer than the typical dominant time scales of baroclinic instability in the storm track regions but shorter than the interannual variations caused by changes in surface boundary conditions such as sea surface temperature (SST) anomalies [*Barnston and Livezey*, 1987; *Dole and Gordon*, 1983; *Dole*, 1986; *Pandolfo*, 1993].

The dynamics of atmospheric LFV in general and circulation regimes in particular are the focus of this article. These dynamics have been, and continue to be, the focus of many research studies. While various low-frequency phenomena have been approached using linear methods, the underlying nonlinear nature of the low-frequency flow has received a great deal of interest, driven by the need to understand the dynamics of the largest (planetary) waves and their interaction with the synoptic patterns that are associated with these waves. Linear and nonlinear approaches to LFV have been contrasted in a review by *Ghil and Robertson* [2002]. The current article builds on that review, particularly discussing more recent methodologies and applications.

One overarching goal is to better understand predictability on intraseasonal and interannual time scales. It is in fact argued that large-scale persistent structures associated with this low-frequency variability can have a profound influence on medium- and longer-term weather and climate prediction [*Colucci and Baumhefner*, 1992; *Robertson et al.*, 2015].

The literature on circulation regimes, starting in the middle of the last century, including their derivation, identifcation, and usefulness, is so extensive that it cannot be ignored. It is expected that due to their persistence and recurrence, regimes would explain nonnegligible amounts of atmospheric variability. Flow regimes have been used in weather forecasting and were considered in extending the limits of weather predictability. On regional scales, weather regimes have been used in downscaling to generate data at smaller scales compared to synoptic scales. The issue of climate change has also highlighted the importance of preferred flow regimes and raised questions over how these will respond to external forcing [*Palmer*, 1999; *Corti et al.*, 1999; *Hsu and Zwiers*, 2001; *Christiansen*, 2003]. Last but not least, weather regimes have also been used in model evaluation [e.g., *Dawson et al.*, 2012; *Dawson and Palmer*, 2014].

Given the importance of nonlinearity and the concept of regimes in the midlatitude atmosphere for weather and climate research, and the extensive and scattered body of literature on the topic, we believe that a review on the subject that brings together the different perspectives of the narrative is required. We wish in this manuscript to present and discuss such a narrative. It is not our intention, however, to focus on investigating the strengths and weaknesses of opposite paradigms, evaluating pros and cons, since we believe that still more research is needed (see the last section) to reach, perhaps, a consensus.

The paper is organized as follows. Section 2 presents a brief review of the relevant concepts of large-scale LFV in the northern hemispheric extratropical circulation, while section 3 summarizes a number of theoretical approaches to understand the characteristics of LFV. Both of these sections are very useful background. The statistical and dynamical methods used to define regimes and their properties are detailed in section 4. While this section gives the reader some intuition as to what is meant in practice by regimes, it can be

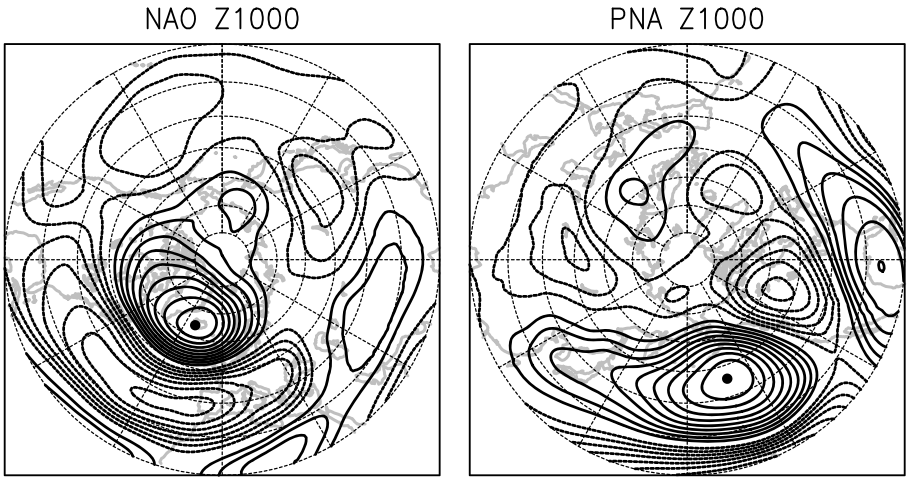

Figure 1. Teleconnection maps obtained from monthly mean 1000 hPa height (Z1000) for boreal winter. The maps indicate the correlation between particular base points (indicated by correlation of 1.0 and the heavy dot) with a high degree of correlation or anticorrelation with Z1000 elsewhere in the Northern Hemisphere. Contour is 0.10. The base points were chosen to agree with those found by *Wallace and Gutzler* [1981] who used sea level pressure. (right) The PNA pattern and (left) the NAO. See text for details.

skipped or referred to later after a reading of the remaining sections. The synoptic interpretation of regimes, focused on the variability of atmospheric jets, is discussed in section 5. Section 6 discusses the ability of weather and climate models to simulate and predict regimes, while section 7 examines how regime properties are useful in understanding the response to external forcing on a wide range of time scales. The utility of the regime approach in synoptic climatology, downscaling, and weather prediction is briefly discussed in section 8. Section 9 gives an outlook for future research.

2. General Features of Low-Frequency Variability in the Northern Hemisphere Extratropics

2.1. Teleconnections

The concept of teleconnections is originally due to *Angström* [1935]: "The weather at a given place is not an isolated phenomenon but is intimately connected with the weather at adjacent places." These large-scale flow patterns are known through their remote effect over wide spatial scales. *Wallace and Gutzler* [1981] pioneered the systematic description of teleconnections, using monthly mean 500 hPa geopotential height fields. They systematically identified widely separated locations whose temporal variations were highly correlated, so that an anomaly at point A is significantly correlated with an oppositely signed anomaly at a remote point B. In some cases the point B anomaly is also significantly correlated with oppositely signed anomalies at remote point C, thus leading to a multicenter pattern with alternating signs, one that can be interpreted as a wave train. Two of the most robust patterns identified this way are the Pacific-North American (PNA) pattern and the North Atlantic Oscillation (NAO) (see Figure 1). The appearance of a high-pressure center in the subtropical Pacific in the PNA is suggestive of tropical forcing, a point we shall develop later. It is a remarkable property of LFV that just a few such teleconnection patterns explain a significant amount of its variability [*Quadrelli and Wallace*, 2004]. These patterns also exert a significant impact on surface weather and seasonal climate conditions [*Plaut and Simonnet*, 2001; *Stan and Straus*, 2007; *Cassou et al.*, 2005] and exhibit variability on intraseasonal as well as interannual and decadal time scales [e.g., *Raible et al.*, 2001].

2.2. Blocking

The midlatitude atmospheric flow is also characterized by other regional features spanning a limited sector of longitude, namely, zonal and blocked flows. Blocking, in particular, can be described as a stationary anticyclone that persists beyond the typical baroclinic instability time scale [*Rex*, 1950a, 1950b, 1961; *Dole*, 1986]. A blocking high often has a nearly barotropic structure with a closed anticyclone at lower levels and a ridge in the upper troposphere, and the jet stream may split into two branches: one poleward of the high and the other equatorward of the cutoff low [*Barry and Carleton*, 2001]. It has been argued that the persistence of blocking is significantly distinct from a simple red-noise model, with the potential for an extension of blocking

predictability [*Dole*, 1986; *Masato et al.*, 2008]. The process of blocking formation is of great interest and has been on the one hand linked to a variety of nonlinear processes, such as the low-frequency advection of vorticity and the convergence of high-frequency (synoptic scale) vorticity flux [*Nakamura et al.*, 1997]. On the other hand, from a linear perspective, the effect of free Rossby waves on blocking is documented by several authors. Rossby waves, which are described in more detail later, can either be free (that is, are linearized solutions to the equations in a basic state representative of the atmosphere) or forced (linearized responses to anomalous forcing of some type). Interference between stationary and traveling Rossby waves can give way to nonlinear processes such as wave breaking [*McIntyre and Palmer*, 1983]. More interestingly, it is argued that free Rossby waves alone may be linked to blocking episodes. For example, some authors have documented frequent association between blocking episodes and westward traveling Rossby waves [*Quiroz*, 1987; *Lejenäs and Madden*, 1992]. The theory behind free Rossby waves is discussed in the next section.

2.3. Grossswetterlagen: True Weather Regimes

Starting from the 1940s, the concept of "weather types" was developed. These are preferred, regional synoptic weather patterns (which may be numerous) known to be common in given geographic regions. A very early example of empirically defined weather types is the *grosswetterlagen*, a catalogue of central European weather types [*Baur et al.*, 1944] maintained by the German Weather Service for over 70 years. This effort, as well as other early classifications of daily circulation patterns over Europe, is well described in *James* [2006]. A recent upsurge of interest in weather classifications has been motivated by their relationship to larger-scale patterns of variability such as teleconnections [*Coleman and Rogers*, 2007; *Roller et al.*, 2016]. Related to weather types, recent work has focused on the effects of European weather patterns on African rainfall [*Polo et al.*, 2011] and on the longer-term forcing of the ocean [*Cassou et al.*, 2011]. Although weather types (generally defined over a region) are not necessarily the same as circulation regimes, the former has inspired the notion of the non-Gaussian nature of atmospheric variability and inspired the early theory of circulation regimes.

3. Theory of Low-Frequency Atmospheric Variability

3.1. Linear, Stochastic Linear, and Nonlinear Approaches

The origins and mechanisms of large-scale and low-frequency variability have been discussed extensively in the literature. It is now recognized that although the spectra of atmospheric variables is typically red, with larger variability at longer time scales, the large-scale tropospheric flow is significantly different from a simple diffusion or red-noise process [*Dommenget*, 2007; *Barnston and van den Dool*, 1993a, 1993b; *Franzke et al.*, 2005, 2007; *Franzke and Majda*, 2006].

Broadly speaking, there are two main streams of thought regarding large-scale low-frequency variability (LFV): the linear and the nonlinear paradigms. The linear approach is based in large measure on the properties of Rossby waves, which owe their existence to the conservation of potential vorticity [*Hoskins*, 1983; *Held*, 1983]. Such waves arise in two forms: as neutral (i.e., not exponentially growing) solutions to the linearized equations of motion without dissipation or forcing, and as orced waves which arise from linear solutions of the same set of equations with external forcing representing, for example, tropical heating.

The linear paradigm, in the presence of symmetric forcing, implies that the dynamics of planetary waves can yield, conceptually, a multivariate Gaussian distribution of the systems probability density function (PDF) [*Leith*, 1973; *Delsole and Farrell*, 1995; *Penland*, 1989; *Penland and Sardeshmukh*, 1995; *Toth*, 1991; *Alexander et al.*, 2008; *Penland et al.*, 2000; *Newman et al.*, 2009]. Linear systems with asymmetric forcing due, e.g., to stabilization by nonlinear processes yield, in general, non-Gaussian probability distribution functions (PDFs) of large-scale variables. Similar non-Gaussian statistics can be obtained with a linear system forced by a state-dependent (or multiplicative) noise [*Sura et al.*, 2005; *Sardeshmukh and Sura*, 2009; *Perron and Sura*, 2013; *Sura and Hannachi*, 2015].

The nonlinear paradigm is based on the concepts of multiple equilibria first mentioned by *Rossby et al.* [1940] and multimodal PDFs. An instructive example of multiple equilibria is given by *Lorenz* [1963], who derived a simple nonlinear low-order dynamical system from a simplified convective model and showed that the dynamics are chaotic where the system trajectory flips unpredictably between two metastable states or regimes. The issue was revived in the early 1970s with the concept of intransitivity [*Lorenz*, 1970], and the suggestion of regimes of internal behavior by *Leith* [1973].

Quoting from *Leith* [1973], "One suggested source of such slow changes is the possible existence of separate regimes of internal behavior such that the atmosphere, having entered one regime, tends to remain

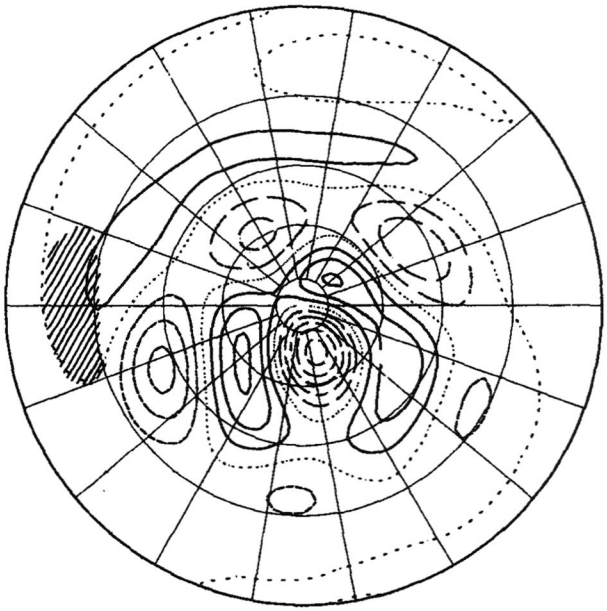

Figure 2. A 300 hPa geopotential height perturbation (contour interval 2 decameter) of a steady state linear solution of a five-layer primitive equation model forced by a deep elliptical heat source at 15°. The hatching represents the region of heating larger than 0.5 K/d. Adapted from *Hoskins and Karoly* [1981].

there for extended periods of time. The long internal time scales induced by such almost intransitive behavior [*Lorenz*, 1970] give a possibility of long-range forecasting skill, especially if the transitions between regimes are predictable."

3.2. Linear Theory: Rossby Waves

The large-scale circulation has connections with, and is affected in important ways by, large-scale (free or forced) Rossby waves of the second class which owe their existence to the conservation of potential vorticity and the resultant exchanges between planetary and relative vorticity [*Rossby et al.*, 1939; *Haurwitz*, 1940; *Deland*, 1964; *Hirooka and Hirota*, 1985; *Madden*, 1978; *Branstator*, 1987; *Kushnir*, 1987; *Kasahara*, 1980; *Alquist*, 1982; *Salby*, 1984; *Lindzen et al.*, 1984; *Madden*, 2007]. These studies suggest that much of the observed large-scale midlatitude flow variability is associated with free and forced Rossby waves. (In contrast, Rossby waves of the first class owe their existence only to gravity and are of less importance in the context of LFV.)

Various free Rossby waves have been identified in the atmosphere. The 5 day [*Deland*, 1964], the 10 day [*Hirooka and Hirota*, 1985], and the 16 day [*Madden*, 1978] waves, along with the Branstator-Kushnir [*Branstator*, 1987; *Kushnir*, 1987] wave, which can be identified with a 25 day free Rossby wave, are among the most well known and most relevant to the large-scale flow. There is evidence that free Rossby waves, particularly those of small zonal wave number and meridional index, do exist and are identifiable in the troposphere. For more details and references on free Rossby waves in reanalyses the reader is referred to the review by *Madden* [2007].

In the linear paradigm, the argument is that Rossby wave theory of linear stationary waves forced by persistent tropical diabatic heating provides the ingredients necessary to explain preferred large-scale flows and their variability [*Hoskins and Karoly*, 1981; *Horel and Wallace*, 1981; *Sardeshmukh and Hoskins*, 1985; *Hoskins and Ambrizzi*, 1993; *Matthews et al.*, 2004; *Seo and Son*, 2012; *Bao and Hartmann*, 2014]. Recently, *Branstator* [2014] demonstrated that transient tropical heating can lead to long-lived midlatitude anomalies. Large-scale midlatitude flows may be essentially steady wave patterns that can be excited on relatively short time scales [*Matthews et al.*, 2004; *Branstator*, 2014] and are stabilized by local midlatitude processes such as transient eddy vorticity fluxes or diabatic heating [*Mitchell and Derome*, 1983; *Shutts*, 1987; *Marshall and So*, 1990; *Adames and Wallace*, 2014; *Lau et al.*, 2012; *Lin et al.*, 2009; *Mori and Watanabe*, 2008; *Molteni et al.*, 2011].

Alternatively, *Frederiksen* [1982], *Simmons et al.* [1983], and *Frederiksen and Webster* [1988], among others [*Simmons et al.*, 1983; *Ding and Wang*, 2005; *Zhang et al.*, 2005; *Zhengyu and Alexander*, 2007; *Quadrelli and Wallace*, 2004; *Winkler et al.*, 2001], have suggested that midlatitude large-scale patterns may result from the instability of spatially varying climatological winter flows to low-frequency perturbations and that patterns generated by this instability may explain persistent large-scale flows.

Stationary forced Rossby waves propagating from the tropics to the midlatitudes can provide the main mechanism for teleconnection [see, e.g., *Hoskins et al.*, 1977]. *Hoskins and Karoly* [1981] used ray theory applied to the linearized five-layer baroclinic model based on the primitive equations [*Hoskins and Simmons*, 1975] on the sphere to explain the atmospheric response to thermal or topographic forcing. They show that the steady linear response to such forcing propagates along great circles or geodesics (Figure 2).

Figure 3 shows a simulated wave train at 300 hPa pressure level obtained from a linearized baroclinic model with a smoothed Earth's orography and winter zonal mean flow background [*Hoskins and Karoly*, 1981].

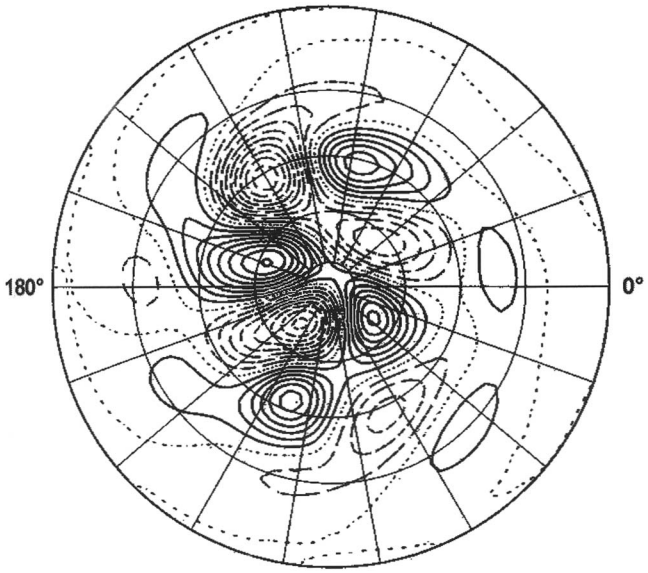

Figure 3. Linearized baroclinic model simulation of a wave train at 300 hPa with smoothed Earth orography and winter mean zonal flow [*Hoskins and Karoly*, 1981].

Interacting Rossby waves can lead to amplification through quasi-resonance [*Petoukhov et al.*, 2013]. It is suggested that this amplification can cause regional weather extremes in the Northern Hemisphere such as the 2013 European floods or the 2010 Russian heat waves [*Petoukhov et al.*, 2013].

3.3. Stochastic Linear Theory

As far as the large-scale flow is concerned, the effect of small-scale disturbances can be regarded as small perturbations or noise that act as forcing. The linearized system can be written in terms of the multidimensional variable **x** as

$$\frac{\mathrm{d}}{\mathrm{d}t}\mathbf{x} = \mathbf{A}\,\mathbf{x} + \boldsymbol{\varepsilon}, \tag{1}$$

where **A** is a linear operator and $\boldsymbol{\varepsilon}$ is the "noise" contribution from unresolved scales and high-frequency waves. The linear operator **A** can always be decomposed into its symmetrical and skew-symmetrical parts, i.e., $\mathbf{A} = \mathbf{A}_s + \mathbf{A}_k$. The operator $\mathbf{A}_s$ yields decay, whereas $\mathbf{A}_k$ yields oscillatory behavior. To ensure stability, the operator needs to have only negative eigenvalues. This can typically be ensured by adding some sort of ad hoc damping [e.g., *Whitaker and Sardeshmukh*, 1988; *Achatz and Branstator*, 1999]. Systematically derived nonlinear dynamic-stochastic models contain the necessary damping in physically meaningful form as nonlinear damping [*Majda et al.*, 1999, 2008, 2009; *Franzke et al.*, 2005, 2015b; *Franzke and Majda*, 2006; *Peavoy et al.*, 2015].

While the model in equation (1) is stable, such a model can still create growth due to the constructive interference of decaying modes, so-called nonmodal growth [*Farrell and Ioannou*, 2000]. For this, the matrix **A** has to be asymmetric or nonnormal. This is the basic idea behind the so-called linear inverse models (LIM) as proposed by *Penland* [1989], *Whitaker and Sardeshmukh* [1988], *Newman et al.* [1997, 2003], and *Winkler et al.* [2001]. That nonmodal growth plays a role in the development of the PNA has been shown by *Cash and Lee* [2001].

The properties of the linear system are determined by the properties of the driving noise. For instance, if the noise is symmetric or Gaussian, then the PDF of the state vector **x** will be symmetric or Gaussian. When the noise is asymmetric, e.g., skewed, the system PDF will be non-Gaussian and asymmetric. Such cases emerge particularly through stabilization by nonlinear processes.

Another method in the stochastic linear paradigm discussed in the literature in the last decade and which leads to nonnormality is multiplicative noise. In this model the noise component due to the contribution from the fast or rapidly decorrelating part depends in a multiplicative manner on the system state:

$$\frac{\mathrm{d}\mathbf{x}}{\mathrm{d}t} = \mathbf{A}\mathbf{x} + \mathbf{B}(\mathbf{x})\boldsymbol{\varepsilon}; \tag{2}$$

see, e.g., *Majda et al.* [2008], *Sura et al.* [2005], *Sardeshmukh and Sura* [2009], and the discussion in *Sura and Hannachi* [2015, and references therein]. The model of equation (2) is of course not entirely linear as the noise is not additive, but the argument is that the large-scale part, on the right-hand side of equation (2), is linear.

Sardeshmukh and Sura [2009], for example, provide a detailed analysis of the application of the model of equation (2) to large-scale flow and derived some of the properties of the skewness (S) and kurtosis (K) of the system PDF. The model they derived is basically linear forced by a correlated additive and multiplicative (CAM) noise. In particular, they show that their model can be used to study weather and climate extremes [*Penland and Sardeshmukh*, 1995; *Sura*, 2011, 2013]. See also the discussion in *Sura and Hannachi* [2015] who provide

a detailed analysis of various sources of non-Gaussianity in the low-frequency and large-scale tropospheric flow. Furthermore, *Majda et al.* [2009] derived the full PDF for the normal form of stochastic climate models. This analytical PDF has a power law component, but its ultimate decay is determined by a squared exponential component which arises from the nonlinear interactions between the slow and fast modes in the climate system.

3.4. Nonlinear Theory

While the linear theory is to some extent successful, it is necessary to consider nonlinear scale interactions in order to fully understand and accurately predict atmospheric low-frequency behavior.

Persistent flow patterns have been explained as multiple quasi-stationary solutions (regimes) in highly truncated nonlinear barotropic systems [*Charney and Devore*, 1979; *Wiin-Nielsen*, 1979]. The idea is that such regimes could be associated with metastable points of the full nonlinear equations. This interpretation was further developed by *Charney and Straus* [1980], *Charney et al.* [1981], *Sutera* [1980, 1986], *Benzi et al.* [1986], *Mo and Ghil* [1987, 1988], and many others. A number of studies [*White*, 1980; *Palmer*, 1999; *Corti et al.*, 1999] suggest that low-order dynamical systems with a regime structure [*Lorenz*, 1963, 1970; *Charney and Devore*, 1979] may present fundamental analogies to the behavior of the atmospheric extratropical large-scale variability. In this simplified nonlinear framework, the atmospheric regimes can be seen as quasi-stationary states or metastable fixed points within the system state space that sporadically attracts the trajectory, hence triggering the recurrent behavior [*Legras and Ghil*, 1985; *Mukougawa*, 1988; *Vautard and Legras*, 1988; *Vautard*, 1990; *Branstator and Opsteegh*, 1989; *Haines and Hannachi*, 1995; *Hannachi*, 1997a, 1997b].

However, this "simple" interpretation is not completely supported by other studies carried out with more realistic models. It has been shown [*Reinhold and Pierrehumbert*, 1982; *Tung and Rosenthal*, 1985, 1986; *Cehelesky and Tung*, 1987; *Majda et al.*, 2006] that in models that also contain faster "weather modes" the regime states do not correspond to the locations of the low-order fixed points. However, many authors have suggested that because flow regimes do attract the system trajectory sporadically to reside within their neighborhood, the resulting persistence of these structures leads to a higher probability of occurrence compared to neighboring flows within the large-scale state space [*Kimoto and Ghil*, 1993a, 1993b]. This can yield in some cases multimodality of the system PDF [*Crommelin*, 2004; *Marshall and Molteni*, 1993].

Diagnosing the attractor in more complex models such as general circulation models (GCMs) and particularly for reanalyses is extraordinarily challenging. (Reanalyses are estimates of the complete state of the atmosphere based on all available observations, as described in the Glossary. For convenience we use "reanalyses" and "observations" interchangeably in this article.) One of the appropriate ways to investigate this is to consider the mean phase space tendencies of the system, which would provide a systematic indication of the presence of nonlinearity. This has, in fact, been done by a number of authors [*Hannachi*, 1997a, 1997b; *Branstator and Berner*, 2005; *Selten and Branstator*, 2004; *Franzke et al.*, 2007; *Kondrashov et al.*, 2011]. These mean tendencies are computed by projecting the tendencies onto the leading empirical orthogonal function (EOF) [*Hannachi et al.*, 2007] and then binning them according to their location in phase space. In a damped linear system these tendencies would point toward the origin. But the analyses performed, e.g., by *Haines and Hannachi* [1995], *Hannachi* [1997a, 1997b], and *Branstator and Berner* [2005], show clear signals of nonlinearity.

Haines and Hannachi [1995] and *Hannachi* [1997a] projected the barotropic vorticity tendency equation onto the space spanned by the leading (up to 10) EOFs of a 10 year perpetual January simulation of the Universities Global Atmospheric Modelling Project (UGAMP) GCM and obtained a zonal flow and a ridge over the Pacific-North America (PNA) sector. *Hannachi* [1997b] extended the analysis by using a two-level baroclinic quasi-geostrophic model. Figure 4 shows these tendencies projected onto the leading two EOFs of the UGAMP GCM stream function field. The singular points or equilibria of the projected dynamics are identified by their zero tendencies. These equilibria correspond to one zonal and two blocking flows over the PNA region [*Hannachi*, 1997b]. In this figure and the next, the rotation of the arrows around the equilibria (marked by dots) represent oscillatory or wave-like flow. Arrows pointing away from an equilibrium indicate instability of that equilibrium and hence an amplifying perturbation. Arrows pointing toward an equilibrium indicate stability and hence a decaying perturbation.

Along the same lines *Branstator and Berner* [2005] computed the mean flow tendencies within the space spanned by the leading EOFs of a very long simulation of the National Center for Atmospheric Research (NCAR) GCM. They identified multiple equilibria in the form of extratropical propagating polar waves in the

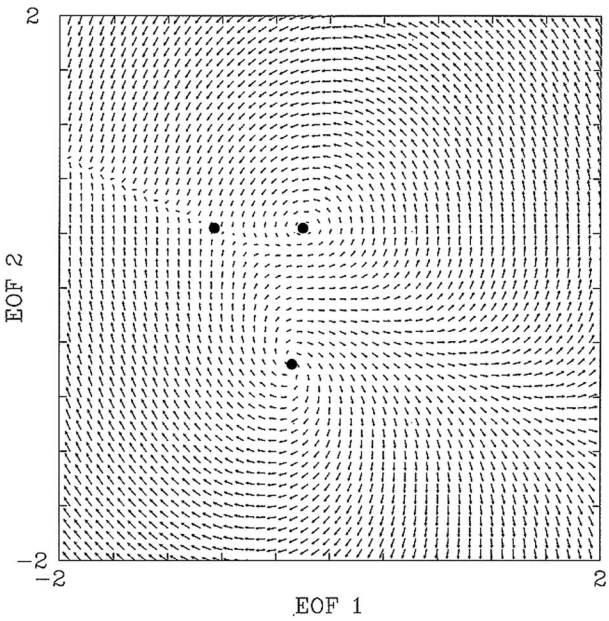

Figure 4. Two-level quasi-geostrophic stream function tendency projected onto the leading two EOFs of the 500 and 250 hPa stream function from the UGAMP GCM simulation. Adapted from *Hannachi* [1997b].

Northern Hemisphere associated with zonal and ridge flows over the western boundaries of the continents. Figures 5a–5d show the flow tendencies within the space spanned by EOF1 and EOF2 (a), EOF1 and EOF3 (b), EOF1 and EOF 4 (c), and EOF2 and EOF3 (d). The location of the singular points representing zero tendencies can be identified. Note that the linear tendencies, obtained by computing the best fit linear flow, have been removed, so that Figure 5 represents only the contribution from nonlinearities. Figures 5e and 5f show the system trajectory generated by the mean flow tendencies within the space spanned by EOFs 1, 2, and 3 (e) and EOFs 1, 3, and 4 (f), suggesting perhaps a homoclinic orbit controlling the dynamics. *Franzke et al.* [2007] have shown that in a quasi-geostrophic model the interactions between the large-scale and smaller scale waves make significant contributions to the nonlinear phase space structure including the transitions between the equilibrium states. Understanding these transitions [e.g., *Deloncle et al.*, 2007; *Selten and Branstator*, 2004; *Franzke et al.*, 2011a, 2011b; *Hannachi et al.*, 2012] is important for weather forecasting [e.g., *Kimoto et al.*, 1992; *Vannitsem*, 2001], but they remain challenging. *Kravtsov et al.* [2005, 2006], for example, suggest that the transition between regimes can be explained by homoclinic orbits.

4. Circulation Regime Methodologies

The notion of regimes is based on two concepts. One is persistence, also called quasi-stationarity, which corresponds to the slowing down of the trajectory in certain regions in phase space. The other is the notion of recurrence, corresponding to the trajectory returning to certain locations (states) more often than would be expected on the basis of multivariate Gaussian statistics. These two concepts, illustrated in Figure 6, are related to the existence of significant deviations of the PDF from multinormal. Figure 6 (left) schematically highlights a trajectory that often returns to states for which the PDF has local maxima but does not linger in these states, while Figure 6 (right) shows part of a trajectory which visits such preferred states and also is nearly stationary. The goals of the methodologies presented here are to identify persistent and recurrent states and relate them to the multidimensional PDF. While all methods identify preferred states, not all methods will be successful in distinguishing unusual persistence from a high degree of recurrence.

4.1. Gaussian and non-Gaussian Properties of the Atmosphere

The non-Gaussian character of large-scale flow was introduced first by *White* [1980], using skewness and kurtosis of the 500 hPa geopotential height field, and later by *Charney et al.* [1981], *Trenberth and Mo* [1985], and others, e.g., *Nakamura and Wallace* [1991] and *Holzer* [1996]. *Toth* [1992, 1993] established the non-Gaussian nature of the northern hemispheric large-scale circulation in boreal winter and showed that the high-dimensional PDF of the daily 500 hPa height field was significantly different from Gaussian, provided that the data were filtered to remove rapidly evolving sequences of states. The empirical studies of *Sutera* [1986], *Hansen* [1986], and *Hansen and Sutera* [1986], and, later, *Hansen and Sutera* [1995], *Cerlini et al.* [1999], *Christiansen* [2005], and *Ruti et al.* [2006], among others, have attempted to show, using low-dimensional planetary wave amplitude information, that some northern hemispheric flow structures occur more frequently than others. This was manifest in the bimodality (the presence of two peaks) in the probability distribution function (PDF) of a one-dimensional wave amplitude index. The statistical significance of the bimodality in the PDF observed in these studies was questioned by *Nitsche et al.* [1994], a major concern

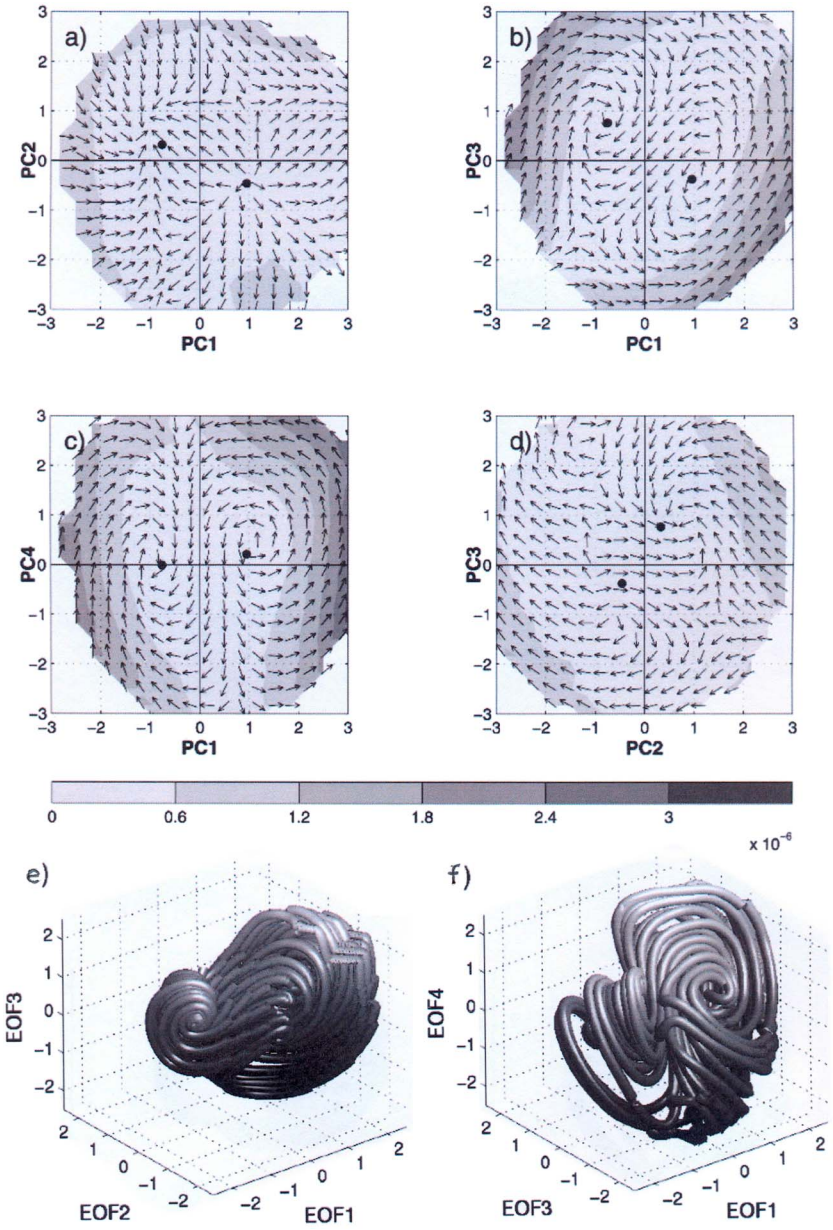

Figure 5. Mean flow tendencies within the (a) EOF1/EOF2, (b) EOF1/EOF3, (c) EOF1/EOF4, and (d) EOF2/EOF3 spaces and the system trajectory generated by the mean flow tendencies within the space spanned by (e) EOFs 1, 2, and 3 and (f) EOFs 1, 3, and 4. Adapted from *Branstator and Berner* [2005].

being the relatively small sample size of available independent observations; see, e.g., *Wallace et al.* [1991], *Stephenson et al.* [2004], *Hsu and Zwiers* [2001], and *Yang and Reinhold* [1991]. *Ambaum* [2008] also suggested that a global measure of wave amplitude is not suitable for multimodality detection as structures at different latitudes are combined.

4.2. Cluster Analysis

Cluster analysis categorizes the entire set of maps into groups with similar characteristics so that these groups are more similar (in some sense) to the others in the same group than to the maps in the other groups. Cluster analysis is a general methodology and can be accomplished using different methods. The most widely used methods in climate research are hierarchical clustering [*Cheng and Wallace*, 1993; *Casola and Wallace*, 2007; *Hannachi et al.*, 2011], *k* means [*Michelangeli et al.*, 1995] and Gaussian mixtures [*Haines and Hannachi*, 1995; *Hannachi*, 1997b; *Smyth et al.*, 1999; *Hannachi and O'Neill*, 2001].

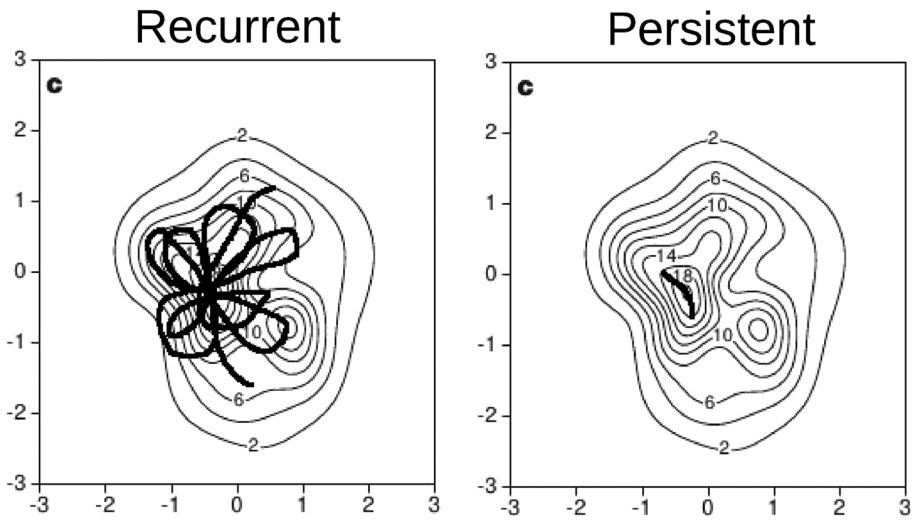

Figure 6. Schematic figure showing the difference between recurrent and persistent regime patterns. (left) The case where the bump in the PDF is caused by the system trajectory crossing this location in phase space very often but without slowing down. (right) The case where the system trajectory slows down in this region of phase space thereby creating the bump in the PDF. Adapted from *Corti et al.* [1999].

In hierarchical clustering, one iteratively combines two of the previous clusters (groups) so that the increase in the within-cluster variance is minimum. The algorithm starts with each map (state of the atmosphere on a given day) defining its own cluster and ends up at the final step with only one cluster. The whole process defines an inverse tree of clusters, going from many branches at the bottom to fewer near the top. The point at which one "cuts" the tree and obtains the final number of clusters may be chosen on the basis of reproducibility [*Cheng and Wallace*, 1993] or the distance between the coordinates of the last set of clusters to be merged [*Toth*, 1993]. The approach of *Cheng and Wallace* [1993] is illustrative of some of the choices that need to be made in applying cluster analysis. These authors start with daily fields of midlevel (500 hPa) geopotential height for boreal winter over the Northern Hemisphere extratropics and remove fluctuations with time scales less than 10 days in order to effectively focus on the LFV (i.e., to minimize the influence of individual synoptic systems). In their analysis of the entire hemisphere, they focus on the final three clusters, obtaining two that are variants of the opposite phases of the PNA and one that is quite similar to one phase of the NAO. (The PNA and NAO are shown in Figure 1). The two PNA-like patterns are not simply the opposite of each other; nor are the NAO-like patterns, something that is often seen in comparing clusters to teleconnection patterns or empirical orthogonal functions (EOFs).

A complementary approach (the so-called *k* means method) seeks to directly partition all states into a fixed, prechosen number *k* of clusters, in a manner which maximizes the ratio *R* of variance among the *k* cluster centroid coordinates (weighted by the population of the cluster) to the average intracluster variance. The centroid coordinates are defined as the average coordinates of all members of the cluster. All coordinates are obtained by projecting the original fields onto a relatively small number *M* (typically 6 to 20) EOFs, thus using the set of *M* principal component time series to define a low-dimensional space. The cluster partition is achieved iteratively: one starts out with *k* seed points and assigns each state to the seed point to which it is closest (according to a measure of distance). Given this initial partition, one recomputes the cluster centroid coordinates, adjusts the partitioning of states into clusters based on the new centroids, and iterates until *R* does not change. Repeating this procedure many times assures that the partition with the highest *R* is obtained. The problem remains of how to choose *k*, the number of clusters. One approach is to define an independent stochastic process (with a Gaussian PDF) for each of the *M* principal components (PCs) in a way that some statistical properties of the corresponding observed principal component are preserved. The cluster analysis is repeated over a large number of trials using synthetically derived data sets (of the same length as the observed) generated from those processes; the percentage of those trials for which the ratio *R* is less than that observed gives a confidence level. In this way *Straus and Molteni* [2004] and *Straus et al.* [2007] use a process which preserves the variance and lag-4 day autocovariance of the original PCs (using low-frequency filtered data), while *Straus* [2010] adapts a method suggested by *Christiansen* [2007] to preserve the covariances

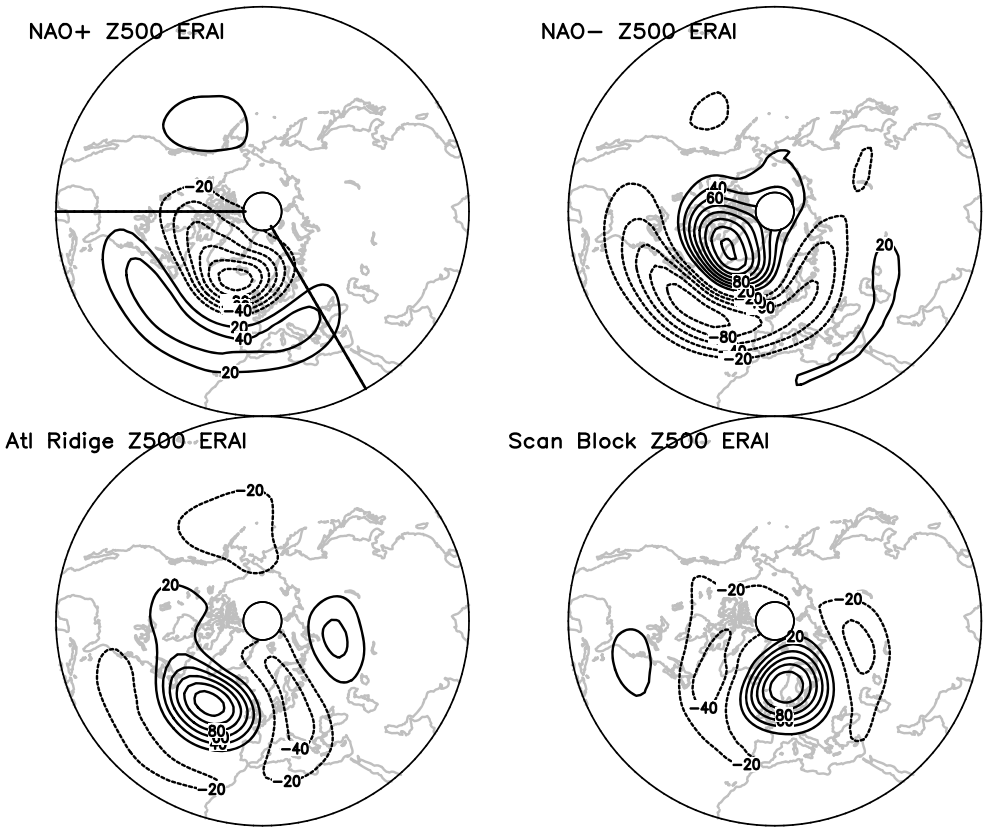

Figure 7. Four clusters obtained for the Euro-Atlantic region (indicated in the top left of each panel) for boreal winter using the *k* means method applied to low-frequency (periods greater than 20 days) 500 hPa geopotential height fields. Regional boundaries indicated by solid lines in upper left panel. Adapted from *Straus et al.* [2017].

at all lags. However, as pointed out by *Christiansen* [2007], this procedure is not sufficient to uniquely determine *k*. Typically, this procedure only suggests a minimum value of *k*. *Straus et al.* [2007] apply this procedure to low-frequency 200 hPa height over the Pacific-North America region and show results for both $k = 3$ and $k = 4$. The variants of the PNA patterns found by *Cheng and Wallace* [1993] are also found here. Over the Euro-Atlantic region, *k* means cluster analysis of low-frequency 500 hPa or 700 hPa height for boreal winter gives a set of patterns for $k = 4$ which are quite robust, even in absence of low-frequency filtering [*Vautard*, 1990; *Cassou*, 2008; *Straus et al.*, 2015]. These patterns, shown in Figure 7, encompass two variants of the NAO of *Wallace and Gutzler* [1981], as seen in Figure 1, as well as two patterns (Scandivanian Blocking and Atlantic Ridge) which suggest persistent large-scale blocking. These latter patterns are *not* meant to summarize the preferred location of blocking but represent large-scale preferred states.

Another method to estimate the number of clusters is the gap statistic [*Tibshirani et al.*, 2001]. The gap statistic is based on comparing the within-cluster dispersion with that from a probability reference model or null distribution, normally taken to be a homogeneous Poisson point process [*Hannachi et al.*, 2011; *Hannachi and Turner*, 2013]. *Hannachi et al.* [2012] applied the gap statistic to the ERA-40 500 hPa geopotential height field over the North Atlantic sector and identified three circulation regimes that are consistent with the preferred positions of the eddy-driven jet latitude [*Woollings et al.*, 2010b].

4.3. Direct Estimation of the Probability Distribution Function

More direct approaches to relating the nonnormal aspects of the atmospheric PDF to preferred states include estimating statistically significant departures of a low-dimensional PDF (in PC coordinates) from a Gaussian PDF [*Kimoto and Ghil*, 1993a; *Corti et al.*, 1999] or finding maxima in the angular PDF *Kimoto and Ghil* [1993b]. The angular PDF is obtained by projecting the entire *M*-dimensional data set (expressed in terms of PC coordinates) onto an *M*-dimensional hypersphere of radius 1. Curves in the $M-1$ dimensional space that encompass local maxima are then found by a "bump-hunting" algorithm. Both approaches have a number of aspects in common with the previously defined methods. They involve prefiltering of the data to retain only the slowly

varying components of the flow, that is, periods when the fields change slowly, and reduction of dimension (usually to two) in principal component space. Statistical testing is also done by comparison with PDFs obtained from samples of synthetic data in which each PC is independently generated from an appropriate stochastic process with a Gaussian PDF. The low-dimensional PDFs are constructed from the discrete points representing the observed or synthetic data set by use of a kernel density estimate [*Silverman*, 1986], in which each point is replaced by a localized distribution in the low-dimensional space, the degree of smoothing being determined by a parameter; the larger the parameter, the fewer local maxima are seen. In *Corti et al.* [1999] this parameter is chosen to be large enough to reject most local (spurious) maxima that appear in the synthetic data due to sampling. In *Kimoto and Ghil* [1993a], the value of the probability at the maxima that appear in the smoothed observed PDF needs to be larger than the probabilities appearing at that point in most synthetic samples for significance. It is noteworthy that the four maxima found by *Kimoto and Ghil* [1993a] over the northern hemispheric domain correspond to maps of height that encompass the NAO and PNA patterns similar to those of *Wallace and Gutzler* [1981], and as in *Cheng and Wallace* [1993] the positive and negative versions of these patterns are not identical.

The results of *Corti et al.* [1999] have proven to be controversial. In particular, the statistical significance of multimodality they find has been disputed [*Stephenson et al.*, 2004]. We bring this point up because *Corti et al.* [1999] use monthly mean data, whereas most of the previous studies quoted retain periods longer than about 10 days and are able to demonstrate statistical significance. Since the typical lifetime of a regime is considerably less than a month, monthly means will smear out the regime signal, as well as provide fewer data samples.

4.4. Mixture Model Method

The methods described above are essentially static statistical analyses of LFV and lead to the identification of states that are in some sense preferred. In these analyses each individual observed state either is assigned to a cluster or may lie within a preferred region of the PDF or not. The possibility that a particular observed state may be associated with more than one preferred state, with different probabilities being attached to these identifications, is not considered.

The mixture model method overcomes this limitation. The approach is to model a univariate or multivariate PDF as a finite sum of component PDFs, each component being Gaussian. This means that the PDF at *each* observed state, expressed in terms of the M PC coordinates, where M as before may be as low as 2, is written as a weighted sum of k Gaussian component PDFs, each component having its own associated mean and covariance matrix. (We choose k as the number of Gaussian components, just as k was chosen as the number of clusters in the k means method.) The weights then give the probability that the observed state will belong to a particular Gaussian component. The parameters to be chosen for the components are then kM coordinates for the mean of each component and $kM(M+1)/2$ parameters for the k symmetric covariance matrices. The weights and parameters can be chosen efficiently using the expectation-maximization (EM) algorithm [*Haines and Hannachi*, 1995; *Hannachi*, 1997b; *Smyth et al.*, 1999; *Hannachi and O'Neill*, 2001]. Note that for a given k, the number of parameters used to fit the observed states ($kM + kM(M+1)/2$) is larger than for the k means method (where essentially only kM parameters, the cluster centroid coordinates, are chosen). As a result, studies using this method [e.g., *Hannachi*, 2007, 2010; *Hannachi et al.*, 2011; *Woollings et al.*, 2010b] tend to find a smaller value of k.

4.5. Tendency Minimization

Another method to identify persistent states is to look for states whose central tendency is close to 0 [*Vautard*, 1990; *Michelangeli et al.*, 1995; *Haines and Hannachi*, 1995; *Hannachi*, 1997b]. A direct computation of states corresponding to the lowest tendencies of filtered 700 hPa height during boreal winter was undertaken by *Vautard* [1990]. As with previous studies, the data are filtered to retain only periods greater than 10 days and reduced in dimensions by retaining only the leading nine PCs. A direct estimate of the states with local minima in their 24 h tendencies (over the Euro-Atlantic region) identified four states, which are similar (but not identical) to the four regimes represented in Figure 7.

This method can be applied more directly to models which use simplified dynamics [*Itoh and Kimoto*, 1996, 1997, 1999; *Sempf et al.*, 2007a, 2007b; *Itoh et al.*, 1999]. For example, *Itoh and Kimoto* [1996], using a simplified two-level quasi-geostrophic model, identified regions of the dynamical attractor in which LFV is dominant. These attractors keep their identity over a wide range of model parameters. " … when some parameters are changed to make the system more turbulent … the system starts transiting among the ruins of the attractors

that used to be stable, a behavior reminiscent of the transitions among different flow regimes in the real atmosphere." This is termed *chaotic itinerancy*. In this model the fully developed flow is characterized by periods of slow change in one configuration, followed by rapid change to another configuration.

4.6. Self-Organizing Maps

The weather regimes paradigm essentially attempts to explain the atmospheric large-scale and synoptic flow in terms of a small number of discrete circulation states. A similar, but not identical, way to look at large-scale weather/climate variability has been used recently based on self-organizing maps (SOM). SOM, also known as Kohonen map [e.g., *Kohonen*, 2001] is an unsupervised neural network method. It attempts to project the high-dimensional data onto a usually two-dimensional space, or grid of ordered patterns, where similar patterns are normally placed next to each other on this grid. In brief, the method is a topology-preserving technique as it attempts to preserve the neighborhood relations of the data. The number of maps to be used, governed by the size of the grid, must be chosen a priori. Many of the applications of SOMs use 10 to 20 ordered patterns, thus describing atmospheric variability in more detail than is typical of cluster analysis applications.

A number of atmospheric researchers have used SOM to describe synoptic circulation patterns using sea level pressure (SLP) [*Hewitson and Crane*, 2002; *Cassano et al.*, 2006; *Reusch et al.*, 2007; *Schuenemann and Cassano*, 2010; *Johnson and Feldstein*, 2010]. *Huth et al.* [2008] provide a review on SOM classification of atmospheric large-scale circulation patterns. For example, *Polo et al.* [2011] used SOM to study the link between the Euro-Atlantic weather regimes and summer West African rainfall, whereas *Polo et al.* [2013] investigated the link between the frequency changes of these regimes and the Mediterranean temperature. Their results seem to indicate a link between dry and wet years and the phase of the NAO and also suggest that weather regimes' frequency is likely to be modulated by Mediterranean temperature extreme conditions.

4.7. Advanced Methods

Statistical methods to estimate persistent regime states include hidden Markov models (HMM) [*Majda et al.*, 2006; *Franzke et al.*, 2008, 2011a; *Franzke*, 2013] and finite element clustering (FEC) [*Horenko*, 2010; *Metzner et al.*, 2012; *Franzke et al.*, 2009; *O'Kane et al.*, 2013; *Risbey et al.*, 2015; *Franzke et al.*, 2015a]. The major advantage of the HMM method is that it simultaneously estimates a Gaussian mixture model (see section 4.4) and the most likely temporal sequences of the regime states, the so-called Viterbi path. Hence, it looks for not only regions in phase space which are very often visited but also how long it stayed in those regions. In a HMM the Viterbi path evolves according to a Markov model [*Rabiner*, 1989]. Persistent states are then identified when the Markov transition matrix is metastable, i.e., when its eigenvalue spectrum has a significant gap [*Franzke et al.*, 2008, 2011a]. Because a HMM amounts to a model reduction (i.e., a high-dimensional field is reduced to a one-dimensional time series), it can be affected by memory effects, so its Markovian structure needs to be checked. This is done by examining the eigenvalues of the HMM transition matrix for different time steps. For Markovian systems the eigenvalues are independent of the time step [*Franzke et al.*, 2008, 2009]. *Franzke et al.* [2009, 2011a] present a way of how to deal with non-Markovianity.

The FEC technique is more general than the HMM and does not make any assumption about the dynamic evolution of the Viterbi path. Furthermore, the FEC method also allows for the dynamic evolution within a regime state by assuming that the system evolves according to a vector autoregressive process of order p with external factors (often referred to as VARX(p)). In a standard HMM the observable variable is assumed to be conditionally independent; i.e., it is a random draw from a Gaussian distribution whose parameters depend on the regime state.

The FEC method is able to detect nonstationary changes in the regimes. *O'Kane et al.* [2013] find that the regime structure of the Southern Hemisphere has changed over the last few decades. Furthermore, *Franzke et al.* [2015a] used FEC to attribute the causes of the recent trends in the Southern Annular Mode (SAM) and Southern Hemisphere (SH) blocking. They show observational evidence that anthropogenic greenhouse gas concentrations have been the major driver of these trends in blocking and the SAM by considering all seasons. This is in contrast to most modeling studies which focus mainly on the austral summer season. The results of *Franzke et al.* [2015a] indicate that the recovery of the Antarctic ozone hole might less strongly delay the signal of global warming. Their results also show that effects from all seasons are likely crucial in understanding the causes of the observed SH secular circulation trends.

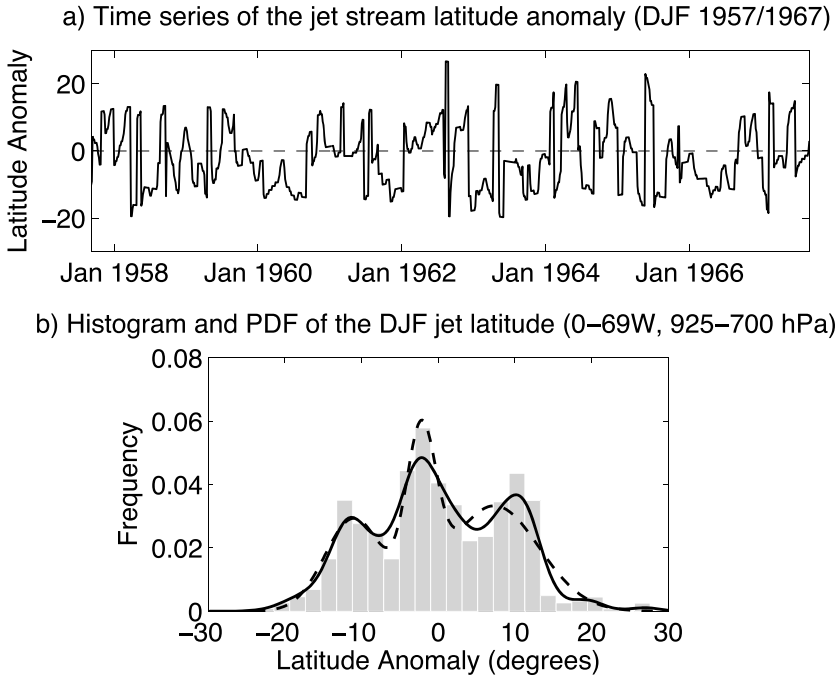

Figure 8. (a) Eddy-driven jet stream latitude from ERA-40 over the North Atlantic during the period December-January-February 1957/1967, and (b) the histogram of the jet latitude along with a three-component mixture model (dashed) and the kernel density PDF estimate (solid). Adapted from *Hannachi et al.* [2012].

5. Synoptic Interpretation of Regimes

In this section we relate the typical results of regime analyses to commonly known midlatitude flow features. Blocking, as described in section 2.2, is a prime example of a familiar flow pattern. Regime analyses very often identify strong anticyclones in the European and Alaska sectors, and these are clearly related to blocking. However, a plethora of blocking indices exists with different attributes, and depending on the blocking index used the resulting events are not always tightly coupled to the regimes identified by a statistical method [*Stan and Straus*, 2007].

Other regime patterns are typically centered over the ocean basins and resemble teleconnection patterns such as the PNA and NAO (see Figure 1). These patterns largely reflect variations in the jet streams, which are a major source of atmospheric variability on all time scales longer than a few days [*Athanasiadis et al.*, 2010]. Dominant shifts of the jet streams arise from a positive feedback between the mean flow and the transient eddies [e.g., *Thompson et al.*, 2002; *Lorenz and Hartmann*, 2003; *Vallis and Gerber*, 2008]. *Feldstein* [2000] showed that the intrinsic time scale of jet stream patterns such as the NAO is of the order of 10 days. Hence, the dominance of a few persistent regime patterns suggests the existence of preferred, persistent jet states on this time scale.

Attention has, therefore, focused on synoptic time scales in understanding the dynamics of such patterns, in particular, the importance of Rossby wave breaking [e.g., *Benedict et al.*, 2004; *Franzke et al.*, 2004; *Rivière and Orlanski*, 2007; *Martius et al.*, 2007]. A general conclusion is that breaking south of the jet (typically anticyclonic breaking) acts to push the jet to the north, while breaking to the north (typically cyclonic) acts to push it south. The PNA pattern, for example, can be understood as a combination of wave breaking-driven jet changes over the Pacific and a subsequent influence on downstream wave development [*Franzke et al.*, 2011b].

Focusing on the wintertime North Atlantic, *Woollings et al.* [2010b] developed a daily metric of the eddy-driven jet latitude. The distribution of jet latitude exhibits a trimodal regime structure, with three preferred jet positions (south, central, and north), which are related to changes in Rossby wave breaking [*Franzke et al.*, 2011b]. There is good agreement between the events identified through the jet and blocking indices [*Woollings et al.*, 2008] and those identified as regimes by a statistical mixture model [*Hannachi et al.*, 2012] or hidden Markov model [*Franzke et al.*, 2011b]. Figure 8 shows an example time series of the winter eddy-driven jet stream

latitude (Figure 8a) along with the histogram and two PDF estimates based respectively on the kernel method and a three-component Gaussian mixture model applied to geopotential height fields (Figure 8b). The potential for predictability is clearly enhanced by the persistence of jet regimes [*Frame et al.*, 2011]. Additional potential comes from the existence of preferred transition pathways between regimes, which generally reflect a preference for poleward propagation of the jet [*Franzke et al.*, 2011b; *Hannachi et al.*, 2012].

The corresponding linear description of this variability uses the NAO and East Atlantic (EA) teleconnection patterns [*Wallace and Gutzler*, 1981]. However, patterns such as this are not able to separate different physical jet changes [*Monahan and Fyfe*, 2006], and hence the different regimes typically project onto a combination of the NAO and EA [*Woollings et al.*, 2010b]. The central jet regime is of interest in comparing the linear and nonlinear views. In this regime, the jet latitude is close to its climatological value, hence representing the undisturbed state of the system. However, the associated flow fields such as geopotential height still exhibit marked anomaly patterns. There is, therefore, a nonzero distance in state space between the mean state of the system and the most frequented state, and this reflects the overly smoothed nature of the Eulerian time-mean flow, in which the jet stream is very broad and weak [*Swanson*, 2001].

Although the Southern Hemisphere has received less attention in the literature, there is also evidence of regime behavior there [*Farrara et al.*, 1989; *Koo et al.*, 2002; *Itoh et al.*, 1999; *Solman and Mendez*, 2003; *Yoden et al.*, 1987; *Robertson and Mechoso*, 2003; *O'Kane et al.*, 2013; *Franzke et al.*, 2015a]. Some of these studies focused on zonal wind variations associated with the jet [*Itoh et al.*, 1999; *Koo et al.*, 2002] and noticed a bimodal distribution in relation to the midlatitude jet vacillation [e.g., *Yoden et al.*, 1987; *Koo et al.*, 2002]. These suggest two regimes, corresponding to a single jet structure dominated by the subtropical jet (at the tropopause) and a double jet structure which also features a stronger polar night jet extending down to the surface.

6. Regimes in Weather and Climate Models

Multiple flow regimes have been identified from a hierarchy of models ranging from highly simplified simple barotropic channel models [*Charney and Devore*, 1979] and spherical barotropic models [*Legras and Ghil*, 1985; *Crommelin*, 2003] to simplified baroclinic models [*Charney and Straus*, 1980; *Reinhold and Pierrehumbert*, 1982; *Achatz and Opsteegh*, 2003] and complex baroclinic models [*Sempf et al.*, 2007b] as well as quasi-geostrophic models [*Yang et al.*, 1997; *D'Andrea and Vautard*, 2001, 2002]. For some models, the regimes were identified as weakly unstable steady states or chaotic itinerancy [*Itoh and Kimoto*, 1996, 1997, 1999; *Sempf et al.*, 2007a, 2007b; *Itoh et al.*, 1999]. Flow regimes have been identified from general circulation models [*Branstator and Berner*, 2005; *Berner*, 2005; *Berner and Branstator*, 2007; *Haines and Hannachi*, 1995; *Hannachi*, 1997a, 1997b] and complex climate models [*Hannachi and Turner*, 2008; *Monahan et al.*, 2000; *Hsu and Zwiers*, 2001; *Handorf et al.*, 2009; *Straus and Molteni*, 2004; *Straus et al.*, 2007; *Kageyama et al.*, 1999; *Corti et al.*, 2003; *Weisheimer et al.*, 2001]. The data used in regime diagnostics can be either unfiltered [e.g., *Smyth et al.*, 1999, H07] or low-pass filtered [e.g., *Toth*, 1991, 1992, 1993; *Kimoto and Ghil*, 1993b; *Itoh and Kimoto*, 1999; *Casty et al.*, 2005; *Straus et al.*, 2007]. The argument in the latter case is that low-pass filtering can better isolate quasi-stationary periods.

The existence of weather regimes has wide implications for the climate system. There is evidence that in a dynamical system with regime structure, the time-mean response of the system to some imposed forcing is in part determined by the change in frequency of occurrence of the naturally occurring regimes [*Palmer*, 1999; *Corti et al.*, 1999]. This is discussed further in section 7. *Corti et al.* [1999], for example, applied a kernel smoothing and identified four hemispheric regimes among them the cold ocean warm land (COWL) pattern associated with low- and high-pressure anomalies over the extratropical land and ocean, respectively (their cluster A). As such, a model which fails to simulate observed regime structures well could qualitatively fail to simulate the correct response to this imposed forcing. The correct representation of weather regimes, their spatial patterns, and persistence properties is therefore essential for a general circulation model (GCM) to properly simulate climate variability and its long-term changes. These motivations have led to the use of flow regimes for the evaluation of climate models [*Weisheimer et al.*, 2001; *Hannachi and Turner*, 2008; *Handorf and Dethloff*, 2012; *Davini and Cagnazzo*, 2014].

A good agreement between simulated and observed Northern Hemisphere weather regimes was found by *Corti et al.* [2003]. These authors applied the same diagnostics described in *Corti et al.* [1999] to the monthly mean values of Northern Hemisphere extended winter 500 hPa heights fields of a 200 year control integration of a coupled GCM and found that the model is able to reproduce patterns of variability consistent with the

observed ones (*Mo and Ghil* [1988], *Cheng and Wallace* [1993], and *Corti et al.* [1999], among others). However, in the model simulation the frequency of COWL (cluster A in *Corti et al.* [1999]), associated with a strong jet stream displaced southward of its climatological mean latitude over the central Pacific and a maximum of the westerlies along the node in the North Atlantic dipole pattern, is overestimated. On the other hand, *Hsu and Zwiers* [2001] noticed that given the relative shortness of the observed record, the COWL pattern is the most significant in the observations and they argued that a sectorial analysis of patterns of natural variability might be more suitable for a proper detection of circulation regimes.

Straus et al. [2007] studied the circulation regimes in the Pacific-North American (PNA) region for the 18-winter period (1981/1982 to 1998/1999) in National Center for Environmental Prediction (NCEP) reanalyses and as simulated by 55 ensemble members of the atmospheric general circulation model of the Center for Ocean-Land-Atmosphere Studies, forced by observed SST and sea ice. These authors showed that three out of the four observed clusters (the Alaskan ridge, Arctic low, and Pacific trough) have identifiable counterparts in the model simulations, while the Arctic high is not well simulated. The relative frequency of occurrence is fairly well reproduced, with the small differences between NCEP and simulated frequencies lying well within the expected spread due to sampling error.

The simulation of weather regimes over the PNA region has been recently studied by *Weisheimer et al.* [2014] using the European Centre for Medium Weather Forecast (ECMWF) coupled seasonal forecasting system (System 4) over the hindcast period 1981–2010. The circulation regimes detected in System 4 are remarkably similar to those of the ERA-Interim reanalysis in the common period, indicating that the ECMWF coupled system is able to reproduce the spatial structure of the flow regimes in the PNA sector. The same results, in terms of weather regimes structure, were found when the experiment was repeated using a version of System 4 in which the Stochastic Physics parameterization [*Buizza et al.*, 1999] was switched off. However, despite the good agreement between observed and simulated spatial patterns, there are in both sets of integrations nonnegligible differences between the observed and the simulated regime frequencies. In particular, the average frequency of occurrence of the particular regime sensitive to El Niño–Southern Oscillation (ENSO) (i.e., the Pacific trough) is strongly overestimated when the stochastic physics parameterizations are not included. This overpopulation indicates that the ECMWF coupled system is too sensitive to the boundary forcing in the equatorial Pacific. As a consequence of this, the frequency of occurrence of the most ENSO-sensitive regime is overestimated, whereas the frequency of the regimes less responsive to the forcing is underestimated. This result is consistent with the findings of *Christensen et al.* [2015] in the context of the idealized *Lorenz* [1996] system. These authors found that including stochastic perturbations from temporally correlated noise enables the system to explore a larger portion of its attractor, triggering regime transitions toward regimes that were otherwise populated less frequently. It is interesting to note that while the excessive sensitivity of the ECMWF coupled system to the equatorial Pacific SSTs does affect the circulation regime frequencies of occurrence, it does not affect the regime structure per se. The four circulation patterns are very well reproduced in both simulations. This might be further evidence for the suggested paradigm (discussed in section 7) that the time-mean response of a system to some imposed forcing manifests itself through a change in frequency of their naturally occurring quasi-stationary regimes [*Palmer*, 1999; *Corti et al.*, 1999; *Hannachi*, 2007; *Hannachi and Turner*, 2008, and others].

Simulated regional climate regimes over the Euro-Atlantic region very similar to the observed regimes (in terms of patterns, persistence, and frequency) were reported by *Dawson et al.* [2012] using the ECMWF Integrated Forecast System (IFS) for continuous atmosphere-only integrations for the 45 year period 1962/1963 to 2006/2007, forced with observed SSTs and sea ice fields (Figure 9). The model was integrated at a "weather forecast" horizontal resolution (T1279, corresponding to about 16 km grid spacing at the equator). When the same experiment was repeated at "climate" horizontal resolution (T159, corresponding to about 125 km grid spacing), the model did not reflect a realistic representation of regimes (Figure 9). In particular, the low-resolution configuration identifies the positive and negative phases of the NAO as clusters, but the significance of the clusters is low. This indicates that the low-resolution model phase space PDF follows a more multinormal distribution. This result demonstrates the importance of representing small-scale processes for the simulation of large-scale climate. It is likely that the superior performance of the T1279 model configuration results from more realistic orography [*Jung et al.*, 2012; *Berckmans et al.*, 2013] and also from more realistic representation of nonlinear Rossby wave breaking processes, which are known to be important in maintaining persistent anomalies [*Woollings et al.*, 2008; *Franzke et al.*, 2011b]. *Dawson and Palmer* [2014] showed that the same configuration of ECMWF IFS at intermediate horizontal resolution (spectral T511 corresponding to grid

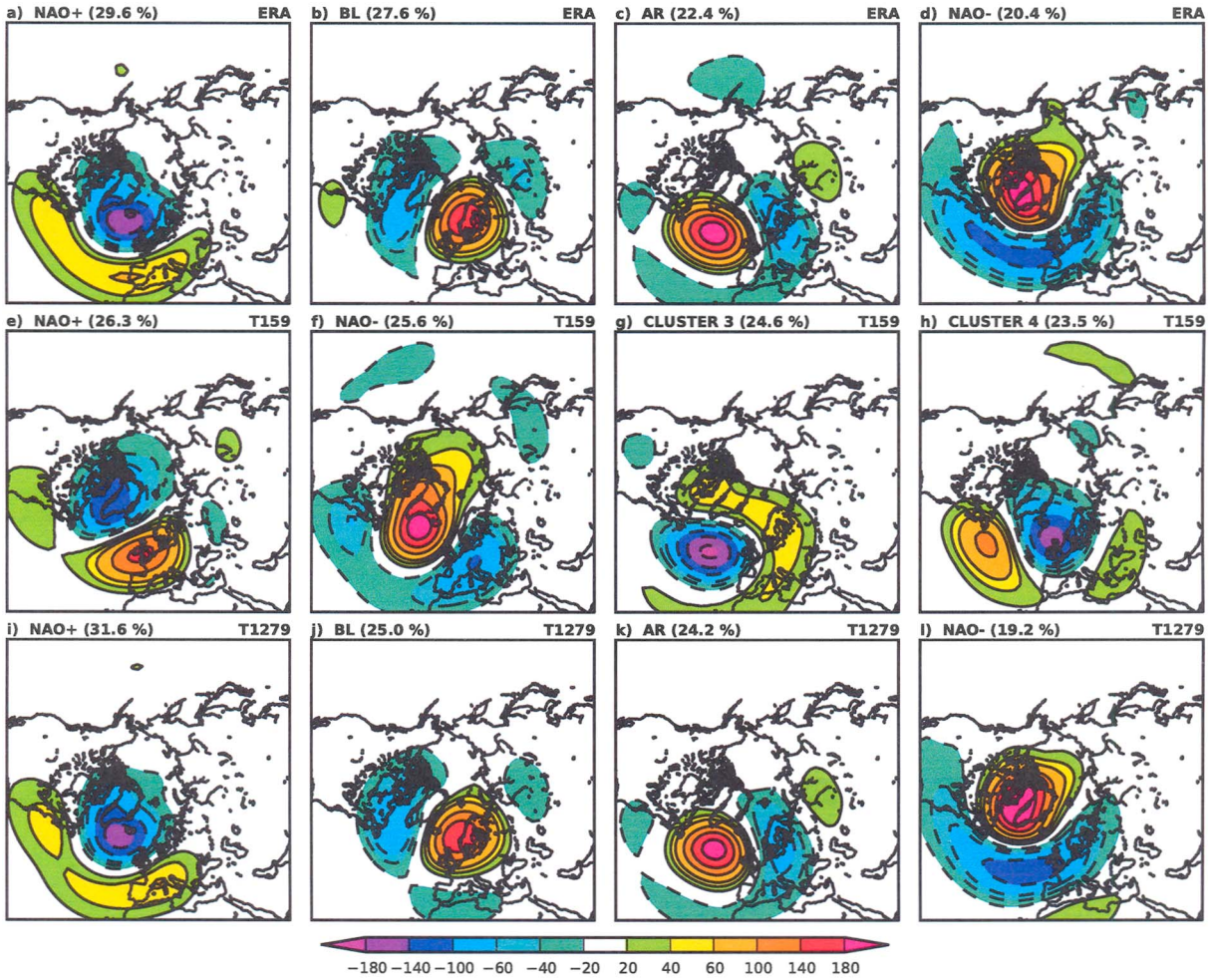

Figure 9. Cluster centroids associated with the regional climate regimes from (first row) ERA-40 and the ECMWF IFS model with resolutions (second row) T159 and (third row) T1279. Negative anomaly contours are dashed. Adapted from *Dawson et al.* [2012].

resolution of 32 km) is able to partially bridge the gap between the very high resolution and the low-resolution configurations, with significant improvements to the climatological frequency of occurrence and persistence of each regime.

These studies have focused on atmosphere-only model integrations, with prescribed SST boundary conditions; therefore, they are not necessarily representative of how the atmosphere may behave in a fully coupled climate model. *Straus et al.* [2007] demonstrated the important role of SST forcing on regime structures, as will be discussed in the next section. It is possible that the consistency of the modeled and observed regimes is in part due to the realistic prescribed SST boundary condition. This suggests that if the SST surface boundary condition provided by a coupled ocean model poorly represents large-scale variability, then it may result in a less realistic atmospheric regime simulation, even at high resolution.

A recent study by *Cattiaux et al.* [2013] highlighted the importance of horizontal and vertical resolution for an accurate simulation of the Euro-Atlantic weather regimes with different versions of the Institut Pierre Simon Laplace (IPSL) coupled models. These authors found that the simulation of weather regimes improves significantly when going from a 96×71, used in the Coupled Model Intercomparison Project version 3 (CMIP3), to a 144×142 (used in CMIP5) resolution. The ability of CMIP3 climate models [*Meehl et al.*, 2007] in reproducing the main features of the jet latitude index probability distributions observed in the reanalyses was investigated by *Hannachi et al.* [2013]. It was found that no model was able to simulate the trimodal behavior of the observed jet latitude distribution (Figure 10). The authors suggest that a possible culprit could be the climatological and seasonal bias of the models' jet latitudes. Many CMIP5 models perform no better (Figure 11),

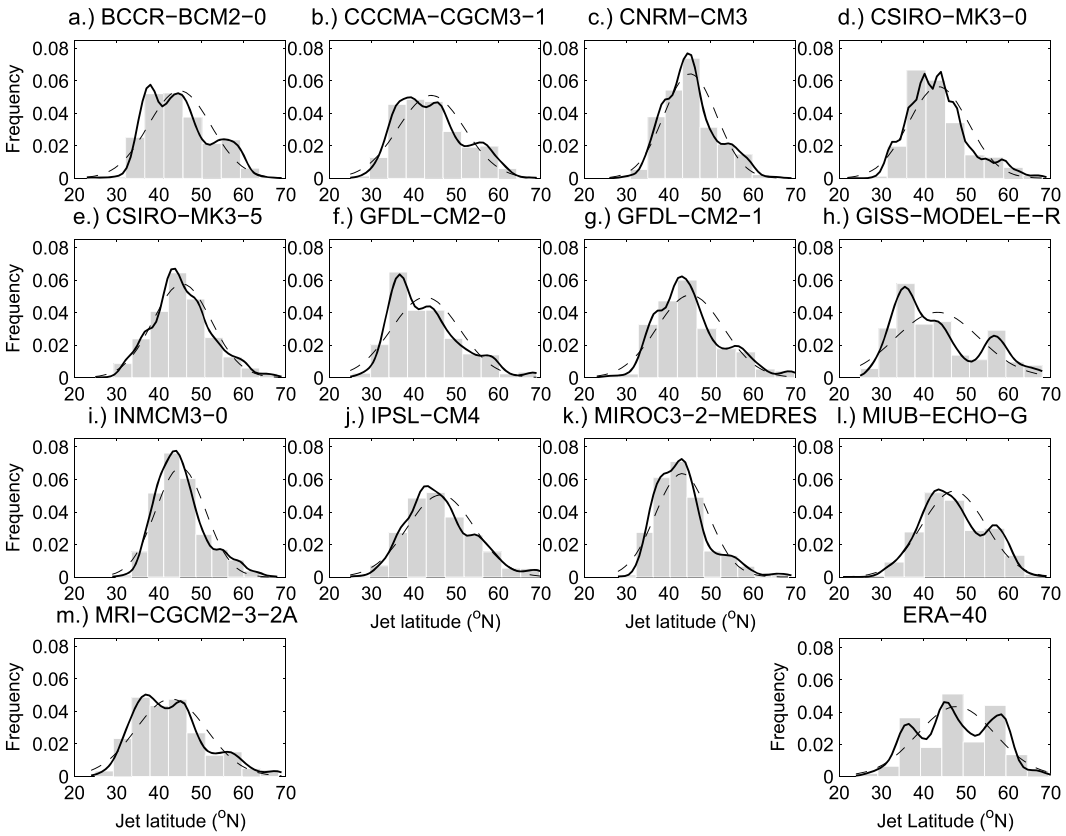

Figure 10. Histograms and kernel PDF estimates of winter (December–March) jet stream latitude time series from a 40 year twentieth century (20C3M) CMIP3 simulation for the period 1961–2000. The same plot from ERA-40 reanalyses is shown in the bottom right corner. Adapted from *Hannachi et al.* [2013].

although a couple now have some structure in their jet latitude distribution resembling the observations [*Anstey et al.*, 2013]. More recent versions of the Met Office model have even clearer structure in the jet latitude distribution even at relatively modest resolutions [*Williams et al.*, 2015]. This suggests that improvements in the accuracy of the numerical schemes can improve regime dynamics without the need for very high resolution or stochastic physics [see *Mitchell et al.*, 2016].

7. Circulation Regimes and External Forcing

The paradigm of preferred states (regimes) of the atmospheric circulation provides an insightful perspective with which to view the effects of "external" forcing, where the definition of external will vary considerably depending on the context. *Palmer* [1993, 1999] argues that the change in the population, or frequency of occurrence, of regimes as a result of external forcing is as important as the mean response.

As a simple example, one aspect of the trend in monthly sea level pressure (hereafter SLP) over the past 50 years or so was the apparent positive trend in the boreal winter North Atlantic Oscillation (NAO) index (defined by the standardized difference in SLP anomaly between the Azores and Iceland) a trend which at the time was suspected to be linked to the increases in greenhouse gases (though over the last 10 years or so the NAO has been either neutral or even negative). However, the set of four regimes generally accepted for boreal winter in the Atlantic region [e.g., *Cassou et al.*, 2004; *Michelangeli et al.*, 1995] yields asymmetric NAO-like regimes, with the regime having decreased midlatitude westerlies (the NAO− regime) shifted westward compared to the regime having increased westerlies (the NAO+ regime). (These regimes were discussed in section 4.2.) The trend in the NAO index can thus be equally well interpreted as an increasing frequency of occurrence of the NAO+ regime.

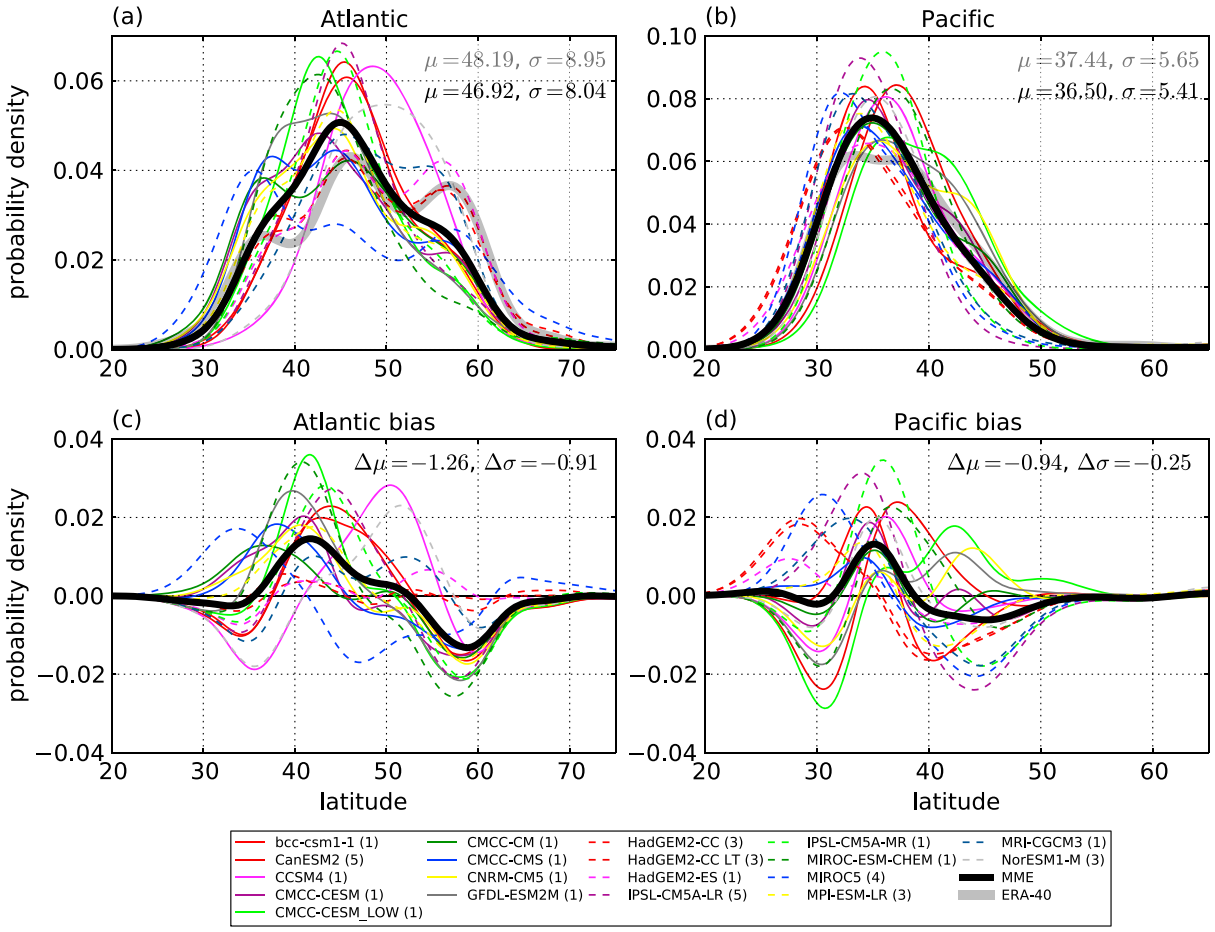

Figure 11. Jet latitude index for the 1960–2000 winter (DJF) period derived from CMIP5 historical model runs over the North Atlantic sector. The same index for the ERA-40 and the multimodel ensemble are also shown in thick gray and thick black, respectively. The (a, b) mean and (c, d) standard deviation of ERA-40 and the multimodel ensemble indices are also shown in the upper right corner. Adapted from *Anstey et al.* [2013].

In this section we discuss the response of regimes to tropical heating on intraseasonal time scales and the response to sea surface temperature (SST) variability on intraseasonal and decadal time scales in some detail. We review studies which make use of the methods described in section 4 in a consistent manner.

There have also been a number of studies which attempt to determine the change in regime properties in climates of the past [*Kageyama et al.*, 1999; *Handorf et al.*, 2009] and in simulated future climates [*Teng et al.*, 2007; *Monahan et al.*, 2000; *Boé et al.*, 2009; *Woollings*, 2008; *Woollings et al.*, 2010a; *Hannachi and Turner*, 2008; *Ullmann et al.*, 2014; *Solman and Le Treut*, 2006; *Branstator and Selten*, 2009]. Since the models used, the experimental design, the number and length of simulations, and the regime analysis methods differed from study to study, it is difficult to compare results and achieve a consistent picture. Hence, we do not review these studies here.

7.1. Forcing of Atlantic Regimes by Subseasonal Tropical Heating

Perhaps the shortest time scale tropical forcing of northern hemispheric midlatitude regimes is that provided by the Madden-Julian Oscillation (MJO), the name given to a broadband oscillation (composed of 20 to 70 day periods) of large-scale convection, embedded in a planetary scale circulation, that propagates eastward near the equator. (For more information on the MJO, see, for example, *Zhang* [2013]). There has been widespread recognition that the occurrence of the NAO, as well as the structure of the Atlantic jet, is influenced by the MJO, as discussed for example in *Ferranti et al.* [1990], *Blade and Hartmann* [1995], *Lin et al.* [2009], and *Yuan et al.* [2011], among many other papers. *Cassou* [2008] examines the MJO influence on the boreal North Atlantic regimes from reanalyses and shows that the NAO+ regime is favored approximately 10 days after the MJO-related convection passes through the Indian Ocean, while the NAO− regime is favored after

the convection has propagated into the western Pacific. The mechanism for the Indian Ocean influence on the NAO+ consists of forced Rossby wave propagation in the Pacific coupled to increased Rossby wave breaking. The favoring of the NAO− regime following western Pacific forcing is hypothesized to involve both changes in the Pacific jet and Atlantic moisture availability.

However, the time lagged effects of the tropical heating in one phase of the MJO (e.g., convection over the Indian Ocean) cannot in principle be cleanly separated from the effects of the MJO heating at a later phase (e.g., convection over the western Pacific) since the MJO phases follow each other quasiperiodically. What is needed is a method of understanding the regime response to the entire cycle of MJO heating. A step in this direction was taken by *Straus et al.* [2015], who added MJO-related diabatic heating (derived from the Tropical Rainfall Measuring Mission satellite data set) directly to the temperature tendencies of each of 48 boreal winter seasonal simulations of the Community Earth System Model (CESM). Since a common time-evolving signal is added to each simulation, the midlatitude response and, in particular, that in the North Atlantic, can be rigorously diagnosed by extracting the evolution of patterns most in common among all ensemble members (i.e., the predictable components [*DelSole and Chang*, 2003]). The leading predictable components of 200 hPa height, the subtropical 200 hPa Rossby wave source [*Sardeshmukh and Hoskins*, 1985], and the 300 hPa height tendency due to synoptic wave vorticity fluxes (a proxy for Rossby wave breaking) depict a highly coherent set of relationships between the MJO-related cycle of tropical heating and cooling, the upper level tropical and subtropical Rossby wave source, and the NAO+ and NAO− regime occurrence. In particular, the NAO+ frequency (which is too low in control CESM simulations) is increased in the MJO heating runs, indicating that the MJO makes a difference in the climatological frequency of NAO+. Figure 12 shows a synthesis of the leading two predictable modes for the total diabatic heating (given in shading), the subtropical Rossby wave source (black contours), the synoptic eddy forcing of the 500 hPa height field at 45°N (blue contours), and the synoptic kinetic energy at 300 hPa between 30 and 50°N (gray contours), all as a function of longitude (abscissa) and time starting on 1 October (ordinate). The synoptic eddy forcing is nearly congruent with the response of the height field, showing episodic NAO+ like responses (positive anomalies) related to the heating. Also shown are the frequency of occurrence of the NAO+ and NAO− clusters based on a cluster analysis of raw daily anomaly fields.

7.2. Interannual to Decadal Response to SST

Possible changes in the structure of regimes of the boreal winter extratropical circulation due to changes in SST forcing were estimated by *Straus and Molteni* [2004, hereafter SM], who analyzed ensemble seasonal simulations with an atmospheric general circulation model (AGCM) carried out for each of 18 recent winters (1981/1982 to 1998/1999), each forced by observed weekly SSTs and initialized from reanalysis. The ensemble size of 55 members for each winter (generated by perturbing the initial conditions) allowed for a full cluster analysis of low-frequency 200 hPa height field in the Pacific-North America region during each winter separately: the analysis of one winter's ensemble incorporated no information from that of any other winter. While many of the clusters found to be significant and robust had similar structure across many of the winters, some were seen primarily during La Niña winters. However, for each ensemble of the three strong El Niño winters within the period, no evidence of significant clustering at all was seen. During these winters the equatorward (and eastward) shift of the Pacific storm track steered disturbances away from the Gulf of Alaska, causing a decrease in the probability of strong blocking in that region and a more homogenous (i.e., unclustered) El Niño "climate". While such an analysis cannot be verified from nature (with an ensemble size of 1), model output can be used in an observational context by providing estimates of the sampling statistics of regimes. *Straus et al.* [2007, hereafter SCM] noted that one of four Pacific regimes obtained from 54 winters of reanalysis (1948/1949 to 2001/2002) which strongly resembles the traditional "PNA" pattern is modified when only the 18 winters (those of SM) of reanalysis was used; the latter pattern more strongly resembles the seasonal mean response to an El Niño event [*Straus and Shukla*, 2002]. The 54 year set of four clusters is significant and robust, but 18 years is far too short a record to yield statistical significance, so an independent assessment of the sampling statistics of clusters is needed. SCM, using the large AGCM ensembles discussed above, showed that the change in structure of the PNA regime was very unlikely to be due to chance and suggested it was due to changes in the nature of the response to El Niño SST anomalies in the more recent period.

A very different approach to relating tropical forcing of Pacific patterns was adopted by *Johnson and Feldstein* [2010], who argue that a continuum perspective for patterns [*Franzke and Feldstein*, 2005] provide a much simpler framework for understanding North Pacific variability. Using daily Pacific SLP for boreal winter from reanalysis (for the period 1958/1959 to 2005/2006), they retain a large number (16) of clusters and use a

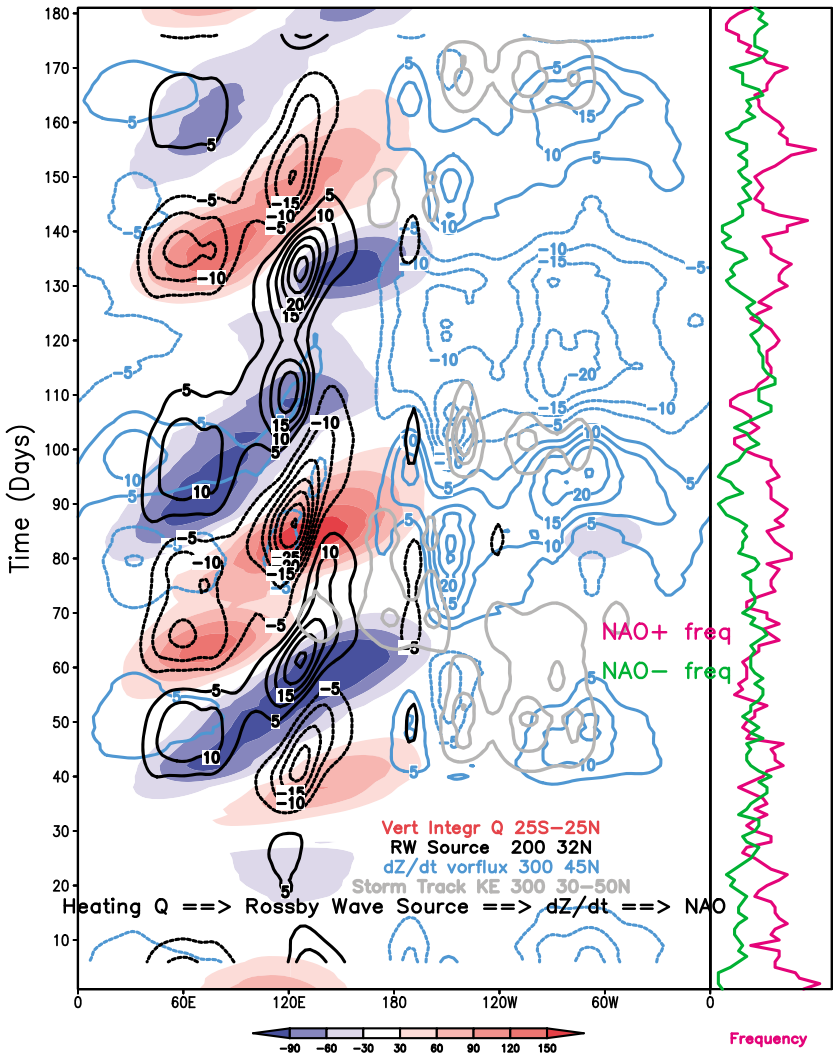

Figure 12. Synthesis of two most predictable components at all times from the MJO intervention of experiments of *Straus et al.* [2015]. Black contours show Rossby wave source at 32°N (interval of 5.0×10^{-11} s^{-1}), blue contours the 300 hPa height tendency from the synoptic scale vorticity flux at 45°N (interval of 5 m d^{-1}), gray contours the synoptic kinetic energy (intervals of 20, 40, and 50 m^2 s^{-2}), and shading the vertically integrated diabatic heating (average 25°S to 25°N, in Wm^{-2}). The red curve on the right shows frequency of occurrence of the NAO+ cluster, the green curve the frequency of occurrence of the NAO− cluster. The abscissa is longitude, and the ordinate is time in days. Adapted from data presented in *Straus et al.* [2015].

self-organizing maps (SOM) approach (discussed in section 4.6) to relate 10 day mean tropical outgoing long-wave radiation (OLR) to the occurrence of the Pacific SLP patterns. They find that five to six PNA-like patterns are found, some of which are related to tropical forcing resulting from Madden-Julian-Oscillation heating, and some of which are related to ENSO. *Bao and Wallace* [2015] also applied self-organized maps to two reanalysis data sets, ERA and NOAA Twentieth Century Reanalysis (20CR), and suggested four reproducible SOM northern hemispheric clusters, namely, the negative NAO, a pattern suggestive of Alaska blocking with a downstream wave train extending over North America and the North Atlantic, an enhancement of the climatological mean stationary wave pattern in the Western Hemisphere that projects positively on the PNA pattern, and a pattern that projects on the negative PNA.

A similar approach was taken by *Fereday et al.* [2008], who use daily SLP in the North Atlantic-European region obtained from a recent surface reanalysis covering the extended period 1870–2002. Clustering algorithms are applied to six nonoverlapping 2 month periods, and 10 clusters are retained. Relationships of these clusters to SST emerge once the SST trend over this long period is removed. Particularly surprising is the difference of the SST-cluster relationship between early and late boreal winter: the November–December season

clusters have the strongest relationship to tropical SSTs. The continuum perspective adopted in these studies is partly motivated by the difficulty in establishing a preferred number of clusters, a result possibly of using unfiltered daily SLP. The rationale and advantages of using prefiltered data, with high-frequency (periods less than 10 days) fluctuations removed, are discussed in *Michelangeli et al.* [1995] and SCM.

In contrast to the above studies, *Cassou et al.* [2004] used classifiability arguments to establish four clusters as the preferred number in the Atlantic during winter, using several long observational records of monthly SLP. Six 30 year integrations of an AGCM with various stationary SST anomalies were used to study the response to Atlantic SST variability: as tropical warm SST anomalies, a midlatitude dipole anomaly, and a sum of the two (tripole anomaly). Experiments with both signs of each anomaly were carried out, along with a control experiment. All seven 30 year experiments were concatenated, and daily SLP was used to derive a single set of four clusters which summarizes all states. The NAO-related clusters were the most sensitive to SST (confirming earlier results of *Terray and Cassou* [2002]), with the NAO+ clusters becoming less frequent during warm tropical Atlantic SST conditions, while the NAO− cluster becomes more frequent. Cold midlatitude SST anomalies severely decrease the NAO+ frequency, while warm anomalies decrease the NAO− frequency.

Also, using a fixed cluster framework for evaluating SST sensitivity experiments, *Robertson et al.* [2000] studied the effect of a positive midlatitude Atlantic SST anomaly in two 10 year runs of an AGCM. Using the low-frequency boreal winter 700 hPa height field from the 100 year control run to establish six preferred regimes, they find that the mean response of one of the runs can be understood as a significant increase in the probability of occurrence of the NAO+ cluster. The anomaly from the second run does not project well onto the control clusters, giving an indication that the anomaly runs are too short (too few) for robust results.

In summary, the mechanisms by which external forcing alters the regime properties depends on time scale. For intraseasonal time scales, the low-frequency variability of the tropical diabatic heating related to the MJO affects the frequency of occurrence of boreal winter Atlantic regimes. On interannual time scales, the change in seasonal mean tropical heating forced by ENSO SSTs alters the frequency of occurrence of Pacific regimes, while Atlantic tropical SST anomalies affect the NAO-related regimes. Midlatitude Atlantic SST anomalies also affect the NAO regimes on interannual time scales, although in the extratropics the atmospheric forcing of the ocean presumably plays a role.

8. Usefulness and Application of Nonlinear Circulation Regimes

As we discussed in the previous section, preferred flow regimes offer an insightful paradigm that can be used to view and measure the effect of external forcing, but of course this is not the only advantage. Nonlinear circulation regimes have been applied to various topics of weather and climate research most notably downscaling and extremes and, to some extent, model evaluation, weather forecasting, and synoptic climatology. Downscaling is required for climate impact assessment and can be classified into three broad categories, namely, dynamical, dynamical-statistical, and statistical. Although dynamical, and to some extent dynamical-statistical, downscaling methods have been used frequently in recent years with regional climate models (RCM), statistical downscaling remains by far the cheapest and most convenient method. Statistical downscaling is, in some sense, the inverse of parameterization used in numerical weather prediction (NWP) [*Enke and Spekat*, 1997]. Downscaling uses large-scale flow features and circulation regimes as predictors to infer smaller-scale processes, notably precipitation and surface temperature at regional and local scales. Parameterization seeks to determine the tendency of large-scale features due to the statistical properties of small-scale convective heating and turbulent damping. Statistical downscaling of precipitation has been obtained using classification [*Goodess and Jones*, 2002; *Vrac et al.*, 2007], fuzzy clustering [e.g., *Bardossy et al.*, 1995, 2002], and classification combined with regression [e.g., *Enke and Spekat*, 1997; *Burrows et al.*, 1995]. Another method based on analogs was presented by *Zorita and von Storch* [1999]. A comparison of techniques for statistical downscaling can be found in *Zorita and von Storch* [1999] and *Tryhom and Degaetano* [2011]. The number of circulation regimes (or patterns) used in downscaling varies across various studies. For example, *Goodess and Jones* [2002] used 14 circulation types based on the NCEP-NCAR SLP to study the relationship to the Iberian rainfall, whereas *Enke and Spekat* [1997] used 10 summer weather patterns to downscale outputs from a GCM over Germany. One of the most significant outcomes of this downscaling exercise is that changes in local and regional weather elements can be (partly) explained by changes in the frequency and/or duration of circulation regimes. Large-scale atmospheric circulation patterns can also be used for ocean downscaling. Winter and summer circulation regimes over the North Atlantic-European region have been used as

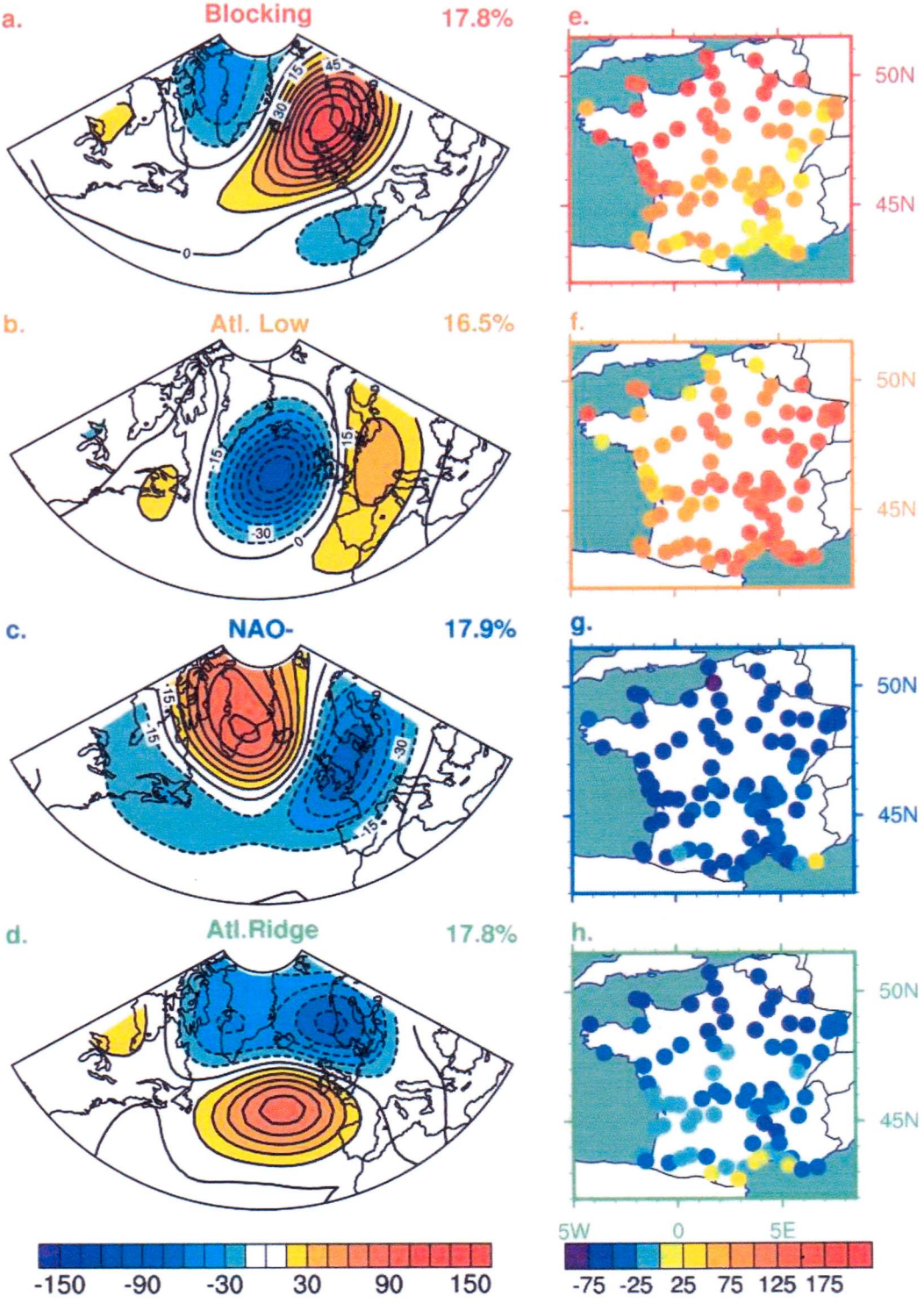

Figure 13. (left column) Summer 500 hPa geopotential height circulation regimes over the North Atlantic-European sector along with their average occurrence for the period NCEP-NCAR 1950–2003. Contour interval: 15 m. (right column) Relative changes (%) in the frequency of extreme warm days for each circulation regime. Adapted from *Cassou et al.* [2005].

predictors to reconstruct ocean surface variables consisting of surface winds and temperature, which are then used to force an ocean model [*Cassou et al.*, 2011; *Minvielle et al.*, 2011].

The link to surface weather and climate extremes is another obvious application of circulation regimes. The consequent persistence of these large-scale and synoptic patterns yields, through a cumulative process of weather fluctuations, an amplitude increase leading thus to extremes [*Fraedrich*, 1990; *Fraedrich et al.*, 1992]. Some authors even suggest some sort of synchronization between resonant circulation regimes and high-amplitude waves [e.g., *Coumou et al.*, 2014; *Petoukhov et al.*, 2013]. *Robertson and Ghil* [1999] used six circulation regimes over the Pacific North America region to study the link to the median as well as extremes of daily surface temperature and precipitation for eight locations within the western U.S. They showed that these extremes are well conditioned by the circulation regimes frequency. They found, in particular, that the PNA and its reverse phase (RNA) are associated with the largest contrasts in local surface temperature and precipitation. In order to partially understand the intense heat waves affecting Europe during the summer of 2003, *Cassou et al.* [2005] determined the relationship between the boreal summer circulation regimes over the Euro-Atlantic regimes and the probability of high surface temperatures, as shown in Figure 13.

A related application of regimes (clusters) to local weather is the endeavor known as synoptic climatology [*Barry and Carleton*, 2001]. Here it is the synoptic weather patterns themselves that are classified into clusters representing preferred synoptic structures. A relatively recent example is the work of *Coleman and Rogers* [2007], who use the long NCEP reanalysis record of daily temperatures, humidities, heights, and winds (at multiple tropospheric levels) as well as sea level pressure over the central United States. Multivariate EOFs are used to determine 10 clusters which define characteristic synoptic weather patterns. These clusters span the seasonal cycle and describe distinctive surface circulations together with baroclinic vertical structures and thermal advection patterns. The authors relate the frequency of occurrence of these weather patterns to large-scale indices, such as the PNA teleconnection index and the Nino3.4 SST index (measuring eastern tropical Pacific Ocean temperatures). Their goal is to provide some predictability of the likelihood of various synoptic situations based on the monthly varying climate indices. A more recent study along the same lines [*Roller et al.*, 2016] focuses on the northeastern sector of the United States. Since certain synoptic conditions are related to human health (via the effects of pollution) and even mortality, the cluster-based approach has an intrinsic societal value.

The study of the association between circulation regimes and surface weather and climate extremes is closely similar to the downscaling procedure discussed above in terms of methodology and scope. This association is addressed mostly through simple conditioning [e.g., *Yiou and Nogaj*, 2004; *Ortiz-Beviá et al.*, 2011; *van den Besselaar et al.*, 2010] or advanced conditioning based on extreme value theory [e.g., *Yiou et al.*, 2008]. There is the suggestion that circulation regimes can modulate the mean and extreme surface weather in a different way [e.g., *Yiou et al.*, 2008]. Through a comparison between the historical and present climate records of the frequency of occurrence of atmospheric circulation regimes, the above association can be extrapolated for future scenario projections to estimate the behavior of future extremes. For example, it is clear that under future climate change scenarios the prevalence of some circulation regimes will likely yield an increase in drought and surface temperature over most southern Europe, the Mediterranean, and northern Africa [*Ortiz-Beviá et al.*, 2011; *Rojas et al.*, 2013; *Driouech et al.*, 2010]. A similar decrease of precipitation over northwestern Europe resulting from anthropogenic emissions was also suggested to be linked to a change in the occurrence of the positive and negative phases of the NAO [*Boé et al.*, 2009]. Note, however, that the usefulness of statistical downscaling in future climate projections has been questioned [*Goubanova et al.*, 2010]. Specifically, the surface impacts of regimes may change in the future, even if the circulation patterns do not [e.g., *Masato et al.*, 2014].

The very nature of the (slowly evolving) large-scale circulation regimes suggests a link to weather forecasting and predictability [e.g., *Ghil and Robertson*, 2002; *Hoffman et al.*, 2005; *Molteni and Corti*, 1998; *Molteni and Tibaldi*, 1990; *Hansen et al.*, 1991]. For example, when a blocking forms over Europe it is likely that it will persist for up to a few weeks, providing thus a window of opportunity to extend the limits of weather predictability. It was already suggested that large-scale quasi-stationary patterns are predictable beyond the "predictability limit" [*Tung and Rosenthal*, 1986]. In this context the preconditioning of the occurrence of Euro-Atlantic regimes by tropical heating discussed in section 7.1 suggests increased predictability in this region if the forecast model can simulate these teleconnections. *Vitart and Molteni* [2010] assess this ability in the ECMWF forecast model. *Chessa and Lalaurette* [2001] find that large-scale circulation patterns are useful in categorizing

forecast skill in the European Centre for Medium-range Weather Forecast (ECMWF) ensemble winter forecasts. More recently, *Ferranti et al.* [2015] used the concept of weather regimes to assess the flow-dependent skill of the ECMWF ensemble predictions over the Euro-Atlantic sector at the late medium range. A targeted clustering product was operationally implemented at ECMWF [*Ferranti and Corti*, 2011]. It summarizes the large amount of information in the Ensemble Prediction System (EPS) providing, for each ensemble forecast, a number of possible synoptic scenarios. Each EPS synoptic scenario is then attributed to a climatological regime [*Michelangeli et al.*, 1995]. This shows the differences between scenarios in terms of the large-scale flow and provides information about the possible transitions between regimes during the forecast. *Ayrault et al.* [1995] also suggest, when characterizing the North Atlantic ultrahigh-frequency variability, that the concept of circulation regimes is central to any statistical approach of European weather. There is evidence that regime patterns allow skillful long-term predictions [*Keeley et al.*, 2009; *Franzke and Woollings*, 2011] of North Atlantic climate though the climate noise amount can be high.

Analyses based on the 500 hPa geopotential heights performed by *McMurdie and Casola* [2009] indicate that weather regimes in the Pacific Northwest affect the forecast errors in the region. They found that the Rocky Mountain ridge regime indicates largest errors of SLP, whereas the coastal ridge indicates largest errors of 2 m temperature. This suggests the possibility of quantifying each regime's forecast performance, as also suggested for the Atlantic jet regimes by *Frame et al.* [2011]. *Langland and Maue* [2012] investigated the forecast skill from multimodel global forecasts and analyses using three operational forecast systems, the ECMWF, NCEP, and the U.S. Navy Operational Global Atmospheric Prediction System. They found that forecast skill from 2007 to 2012 is related to the large-scale atmospheric anomaly flow. Precisely, the anomaly correlation coefficient is found to be significantly correlated with the Arctic Oscillation.

Finally, besides the effect of regimes on local climate [e.g., *Plaut and Simonnet*, 2001; *Simonnet and Plaut*, 2001; *Robertson and Ghil*, 1999] and intraseasonal variability [*Ponater et al.*, 1994] there is also evidence that midlatitude cyclone tracks can be conditioned by large midlatitude flow regimes [*Blender et al.*, 1997; *Gaffney et al.*, 2007]. The recent work of *Catto* [2016] suggests that the different types of cyclogenesis should also be regime dependent. Large-scale flow regimes are also used in weather generation [*Bardossy and Plate*, 1992] and rainfall prediction [*Liu et al.*, 2006] and have also been used to interpret proxy records [*Lorreya et al.*, 2007].

9. Outlook

The extensive body of literature seems to provide evidence in support of the existence of flow regimes in nature, particularly on regional scales. Regimes have also been found in a hierarchy of models, from simplified barotropic and quasi-geostrophic models of the atmosphere to sophisticated weather prediction models to comprehensive coupled ocean-atmosphere climate models. It is also perhaps fair to say, however, that the evidence is not beyond a shadow of a doubt. While many methods for regime detection agree that there is evidence of non-Gaussian behavior to aspects of the large-scale circulation, different approaches (and the same approach used on different atmospheric variables) yield different regime structures. The optimal number of regimes to summarize the observed and simulated non-Gaussian behavior is also uncertain. This points to the need for more research on regime existence and methods of regime identification, given the importance of these structures in atmospheric low-frequency and large-scale behavior.

Flow regimes have been diagnosed on hemispheric as well as regional scales in both hemispheres, although most studies have focused on the Northern Hemisphere during boreal winter. These regimes have been interpreted from various angles, namely, persistence, quasi-stationarity, and intermittency. Flow regimes can be modified by "external" forcing in terms of both frequency of occurrence and structure. There is clear evidence pointing to the link between the eddy-driven jet stream position and flow regimes, particularly on regional scales.

Regime analyses play a key role in complementing linear approaches, as they are able to identify asymmetries in patterns and responses to forcing that linear approaches are not [e.g., *Cassou et al.*, 2004]. The regime paradigm in tropospheric midlatitudes has proved quite useful in weather and climate research on various aspects including predictability, downscaling, present and projected weather and climate extremes, and even paleoclimate proxy verification and reconstruction. In some cases, though, a regime approach has to be taken with care. An obvious example is that sampling uncertainty is often an issue with small data sets. Regime structures can change in response to forcing, and the impacts of a given regime are not necessarily the same under an altered climate.

An important question for future research is how regimes will change in a globally warmer world. There is some evidence that some regime patterns have undergone secular trends [e.g., *Thompson et al.*, 2000; *Franzke*, 2009; *Franzke and Woollings*, 2011], but also, internal variability is high [*Risbey et al.*, 2015]. Accurate future projections of the behavior of regime patterns are needed because of their impact on surface weather and climate. New nonstationary analysis methods or model-based clustering methods [*Fraley and Raftery*, 1998, 2003] are needed. The methods proposed by Horenko and colleagues could be promising in this regard [*Horenko*, 2010; *Metzner et al.*, 2012; *O'Kane et al.*, 2013; *Risbey et al.*, 2015; *Franzke et al.*, 2015a].

Glossary

Additive and multiplicative noise: Additive noise refers to stochastic forcing of a system, which does not depend on the state of the system. When the noise depends on the state of the system, then the noise is multiplicative.

Atmospheric analysis and reanalysis: An atmospheric analysis refers to the best estimate of the state of the atmosphere at a given time based on the objective combination of a network of observations and the results from a numerical model (forecast). The technique used to produce the analysis is called data assimilation and represents the best fit of the numerical model to the available data, taking into account the errors in the models and in the data. An atmospheric reanalysis consists of atmospheric analyses based on historical observational data spanning an extended period, using a single consistent model and data assimilation scheme throughout.

Autoregressive process: A time-varying process, which can be represented by a mathematical model in which the future state of the system depends linearly on its own previous values, plus an additive noise.

Baroclinic instability: A hydrodynamic wave instability associated with vertical shear of mean horizontal wind (equivalently north-south mean temperature gradient) and is characterized by spatial and temporal scales of the order of 1000 km and 2 to 3 days, respectively. It is responsible for the formation (also called cyclogenesis) and growth of midlatitude cyclones.

Barotropic/Baroclinic atmosphere: In a barotropic atmosphere, density depends only on the pressure. In a baroclinic atmosphere, density depends on both temperature and the pressure. In a baroclinic atmosphere, horizontal temperature gradients can exist, fostering baroclinic instability.

Blocking: A midlatitude atmospheric anticyclonic state associated with a persistent quasi-stationary high-pressure system. Typically, there will be reversal of the flow, with easterly winds on the equatorward side of the block. The persistence time varies between several days to several weeks.

Centroid: The centroid of a set points in a n-dimensional space is the mean position of all the points in all the coordinate directions. In the case of clusters, it refers to the center of a cluster state.

Diffusion process: A mathematical model to describe the slow process of mixing by random molecular motion in fluids. Such a model describes, for example, the trajectory of a particle embedded in a fluid and subjected to random displacements due to collisions with molecules.

Downscaling: A method to infer the state of meteorological variables at local scales from the state of meteorological variables at the large scales. Downscaling can be statistical (i.e., based on past observations between large-scale variables and local variables) or dynamical (i.e., where large-scale observations or output from general circulation models are used to drive regional numerical models at higher spatial resolution).

Empirical orthogonal functions (EOFs): EOFs are a set of ordered fields which provide a set of data-dependent basis functions in which to expand a data set (such as daily geopotential height fields). The set of time-dependent coefficients are called the principal components, which serve as a new set of coordinates for the data. The EOFs are the eigenvectors of the symmetric covariance matrix, ordered so that the maximum amount of space-time variance is explained by the fewest modes. The process of obtaining EOFs and principal components is sometimes referred to as "principal component analysis."

ENSO: The El Niño–Southern Oscillation (ENSO) is an irregularly periodic variation in winds and sea surface temperatures (SSTs) over the tropical eastern Pacific Ocean, affecting much of the tropics and subtropics. The warming phase is known as El Niño and the cooling phase as La Niña. The Southern Oscillation is the

accompanying atmospheric component, coupled with the sea temperature change: El Niño is accompanied with high and La Niña with low air surface pressure in the tropical western Pacific.

Extended range forecast: This type of forecast is used to describe the extension of the forecast range beyond the conventional medium range which is of the order of 10–15 days.

Fixed point: A fixed point of a function is an element of the function's domain that is mapped to itself by the function. Fixed points or equilbria are used in dynamical systems to describe a state at which the system becomes stationary, i.e., does not evolve.

General circulation model (GCM): A mathematical representation of the general circulation of a geophysical fluid. It uses the Navier-Stokes equations on a rotating sphere, augmented by an equation for rate of change of entropy and representations of radiation, gravity wave, and diffusion processes to simulate the evolution of the atmosphere and/or the ocean.

Homoclinic orbit: In the phase space of a dynamical system, trajectories converge to a stable equilibrium or fixed point, and they diverge from an unstable equilibrium. For a saddle fixed point there is a trajectory that joins this equilibrium to itself, which is known as homoclinic orbit. It is the intersection between the "set" of trajectories diverging from and the "set" of trajectories converging to the equilibrium. These two sets are known, respectively, as the unstable and stable manifolds of the saddle equilibrium.

Jet streams: These refer to a belt of strong wind, like rivers of wind high in the atmosphere, flowing around the Earth. The major streams on Earth are westerly jets, particularly the subtropical and the eddy-driven jets. The subtropical jet stream is located in the upper atmosphere near the tropopause. The eddy-driven jet, which spans the depth of the troposphere, flows over the middle to northern latitudes in the Northern Hemisphere, while it is circles the Antarctica in the Southern Hemisphere.

Kernel density estimate: This refers to a nonparametric way to estimate the probability density function of a random variable from a finite sample. Each value of the sample, viewed as a delta function of probability, is replaced with a continuous function (the kernel) of unit area centered at that value.

Low-frequency variability: This refers to the time scale of atmospheric variability longer than the synoptic scale of a few days and shorter than one season.

Markov model: A mathematical model in which it is assumed that, given its past history, its future state depends only on the most recent past (and not on the sequence of events that preceded it). It is also known as a first–order autoregressive process.

Metastable (saddle) fixed point: This refers to a fixed point (or equilibrium) of a dynamical system that is stable to some perturbations but unstable to others. For example, a ball sitting on a saddle is in a metastable state hence the "saddle" terminology.

Mountain torques: Mountains constitute stationary obstacles and do exert a kind of "push" or drag on the atmosphere. As the flow is mostly westerly the pressure difference between the eastern and western sides of mountains yields a pressure gradient force in their vicinity, which generates a torque that tends to speed up the Earth's rotation. A similar, but opposite, torque is exerted onto the atmosphere. The mountain, and also frictional, torques provide sources and sinks for the atmospheric angular momentum. It is suggested that changes in the large-scale flow pattern and teleconnection in addition to midlatitude jet intensity are associated with mountain torques.

Neural network: This refers to a procedure or computer model that simulates the behavior of biological neural networks (i.e., an interconnected web of neurons transmitting complex patterns of signals).

Parameterization: In the context of weather or climate models, this refers to the procedure of expressing (or parameterizing) processes that are too small scale or complex to be explicitly represented in the model in terms of other processes which are explicitly resolved within the models (e.g., the large-scale flow).

Planetary vorticity: The vorticity associated with the Earth's rotation around its axis. Planetary vorticity is maximum at the pole and 0 at the equator.

Planetary waves: The largest spatial scale components of the atmosphere's circulation.

Power spectrum: The power spectrum of a time series (or signal) provides a measure of the power (or energy) distribution as a function of frequency. For example, a signal containing a harmonic (or periodic) component embedded in an additive noise has a particularly high power around the harmonic frequency.

Probability density function (PDF): The PDF of an atmospheric variable describes the relative likelihood for this variable to take on a given value. It can be estimated by fitting a distribution over a histogram constructed on the basis of available data. Another common way of estimating a PDF is by the kernel density estimation that uses a kernel (in general Gaussian) to smooth frequencies over the bins.

Red-noise process: A signal generated by a stochastic process with a power spectrum that is weighted toward low frequencies but without a single preferred frequency. Red-noise processes are normally used as a null hypothesis for large-scale atmospheric variability.

Relative vorticity: The vorticity of the rotating flow excluding the planetary vorticity.

Rossby wave: A large-scale wave in the atmosphere (or ocean) owing its existence to gradients in the planetary vorticity (i.e., Earth's rotation). Rossby waves in the atmosphere, associated with pressure systems and the jet stream, affect major weather systems. Oceanic Rossby waves move along the thermocline, i.e., the boundary between the warm upper layer and the cold deeper part of the ocean.

Stable and unstable stationary states: A stable stationary state is also called a fixed point or equilibrium and refers to a stationary (that is time independent) state that has the property that if the system is slightly perturbed away from this state, the system will return to this state. For example, the vertical position is a stable stationary state of a pendulum. An unstable stationary state is likewise a time-independent state, but if the system is perturbed from such a state, this perturbation will grow. For example, a small marble ball sitting precisely on top of a large ball is an unstable stationary state.

Stochastic physics: Parameterization schemes within weather and climate models that include stochastic components to represent the dynamical effects of the unresolved scales.

Teleconnections: Links, often through correlation, between climate anomalies occurring at one specific location and at large distances. They represent therefore patterns connecting widely separated regions. Examples of teleconnections include the North Atlantic Oscillation (NAO) and the Pacific-North American (PNA) patterns.

Troposphere and Stratosphere: The Earth's atmosphere is normally divided into four layers according to the vertical temperature profile. The troposphere is the lowermost layer and is characterized by a decrease of the temperature with height. Most weather systems occur within the troposphere. Moving upward from the troposphere, we find the stratosphere (which is quite stable to small-scale disturbances), mesosphere, and thermosphere.

Tropopause: The upper boundary of the troposphere, i.e., the boundary between the troposphere and stratosphere. The tropopause is a dynamical feature which is temporarily deformed by passing weather systems.

Vorticity: It is defined as the curl of the velocity vector. The term is often used (as in this article) to refer to the vertical component of the vector vorticity and measures the circulation or swirling (rotating) component of the flow. The sum of the relative and planetary vorticities yield the absolute vorticity.

Wave breaking: The process of a wave overturning, which follows wave propagation and amplitude growth. Wave breaks release momentum and energy and lead to irreversible deformation of flow contours.

Acknowledgments

D.M.S. acknowledges financial support from the National Science Foundation (grants ATM-0830062 and ATM-0830068), the National Oceanic and Atmospheric Administration (grant NA09 OAR 4310058), and the National Aeronautics and Space Administration (grant NNX09AN50G). C.F. was supported by the German Research Foundation (DFG) through the cluster of excellence CliSAP (EXC177) at the University of Hamburg. The authors would like to thank the anonymous reviewers for their insightful comments and suggestions that have contributed to improve this paper. The data used to generate Figures 1 and 7 come from the reanalysis data set produced by the National Centers for Environmental Prediction and stored at the National Center for Atmospheric Research (available at rda.ucar.edu/datasets/ds090.0/). All other figures come from published and documented sources.

References

Achatz, U., and G. W. Branstator (1999), A two-layer model with empirical linear corrections and reduced order for studies of internal climate variability, *J. Atmos. Sci.*, *56*, 3154–3160.

Achatz, U., and J. D. Opsteegh (2003), Primitive-equation-based low-order models with seasonal cycle. Part II: Application to complexity and nonlinearity of large-scale atmospheric dynamics, *J. Atmos. Sci.*, *60*, 478–490.

Adames, A. F., and J. M. Wallace (2014), Three-dimensional structure and evolution of the MJO and its relation to the mean flow, *J. Atmos. Sci.*, *71*, 2007–2026.

Alexander, M. A., L. Matrosova, C. Penland, J. D. Scott, and P. Chang (2008), Forecasting Pacific SSTs: Linear inverse model predictions of the PDO, *J. Clim.*, *21*, 385–402.

Alquist, J. (1982), Normal-mode global Rossby waves: Theory and observations, *J. Atmos. Sci.*, *39*, 193–202.

Ambaum, M. H. P. (2008), Unimodality of wave amplitude in the Northern Hemisphere, *J. Atmos. Sci.*, *65*, 1077–1086.

Angström, A. (1935), Teleconnections of climatic changes in present time, *Geogr. Annal.*, *17*, 243–258.

Anstey, J. A., et al. (2013), Multi-model analysis of Northern Hemisphere winter blocking: Model biases and the role of resolution, *J. Geophys. Res. Atmos.*, *118*, 3956–3971, doi:10.1002/jgrd.50231.
Athanasiadis, P. J., J. M. Wallace, and J. J. Wettstein (2010), Patterns of wintertime jet stream variability and their relation to the storm tracks, *J. Atmos. Sci.*, *67*, 1361–1381.
Ayrault, F, F. Lalaurette, A. Joly, and C Loo (1995), North Atlantic ultra high-frequency variability, *Tellus*, *47A*, 671–696.
Bao, M., and D. L. Hartmann (2014), The response to MJO-like forcing in a nonlinear shallow-water model, *Geophys. Res. Lett.*, *41*, 1322–1328, doi:10.1002/2013GL057683.
Bao, M., and M. J. Wallace (2015), Cluster analysis of Northern Hemisphere wintertime 500-hPa flow regimes during 1920–2014, *J. Atmos. Sci.*, *72*, 3597–3608.
Bardossy, A., and E. J. Plate (1992), Space-time model for daily rainfall using atmospheric circulation patterns, *Water Resour. Res.*, *28*, 1247–1259.
Bardossy, A., L. Duckstein, and I. Bogardi (1995), Fuzzy rule-based classification of atmospheric circulation patterns, *Int. J. Climatol.*, *15*, 1087–1097.
Bardossy, A., J. Stehlik, and H. J. Caspary (2002), Automated objective classification of daily circulation patterns for precipitation and temperature downscaling based on optimized fuzzy rules, *Clim. Res.*, *23*, 11–22.
Barnston, A. G., and R. E. Livezey (1987), Classification, seasonality and persistence of low-frequency atmospheric circulation patterns, *Mon. Weather Rev.*, *115*, 1083–1126.
Barnston, A. G., and H. M. van den Dool (1993a), *Atlas of Climatology and Variability of Monthly Mean Northern Hemisphere Sea Level Pressure, 700 mb Height and 1000–700 mb Thickness*, 219 pp., 1950-1992 NOAA Atlas #10, US Dept. of Commerce, Univ. of Michigan, Ann Arbor, Mich.
Barnston, A. G., and H. M. van den Dool (1993b), Towards understanding the causes of low-frequency variability: The inter-annual standard deviation of monthly mean 700 mb height, *J. Clim.*, *6*, 2083–2102.
Barry, R. G., and A. M. Carleton (2001), *Synoptic Climatology*, 620 pp., Routledge, London.
Baur, F., P. Hess, and H. Nagel (1944), *Kalendar der Grosswetterlagen Europas 1881-1939*, DWD, Bad Hamburg.
Benedict, J., J. Lee, and S. Feldstein (2004), Synoptic view of the North Atlantic Oscillation, *J. Atmos. Sci.*, *61*, 121–144.
Benzi, R, P. Malguzzi, A. Speranza, and A. Sutera (1986), The statistical properties of general atmospheric circulation: Observational evidence and a minimal theory of bimodality, *Q. J. R. Meteorol. Soc.*, *112*, 661–674.
Berckmans, J., T. Woollings, M. E. Demory, P. L. Vidale, and M. Roberts (2013), Atmospheric blocking in a high resolution climate model: Influences of mean state, orography and eddy forcing, *Atmos. Sci. Lett.*, *14*, 34–40.
Berner, J. (2005), Linking nonlinearity and non-Gaussianity of planetary wave behavior by the Fokker-Planck equation, *J. Atmos. Sci.*, *62*, 2098–2117.
Berner, J., and G. Branstator (2007), Linear and nonlinear signatures in the planetary wave dynamics of an AGCM: Probability density functions, *J. Atmos. Sci.*, *64*, 117–136.
Blade, I., and D. L. Hartmann (1995), The linear and nonlinear extratropical response of the atmosphere to tropical intraseasonal heating, *J. Atmos. Sci.*, *52*, 4448–4471.
Blender, R., K. Fraedrich, and F. Lunkeit (1997), Identification of cyclone track regimes in North Atlantic, *Q. J. R. Meteorol. Soc.*, *123*, 727–741.
Boé, J., L. Terray, C. Cassou, and J. Najac (2009), Uncertainties in European summer precipitation changes: Role of large scale circulation, *Clim. Dyn.*, *33*, 265–276.
Branstator, G., and J. Berner (2005), Linear and nonlinear signatures in the planetary wave dynamics of an AGCM: Phase space tendencies, *J. Atmos. Sci.*, *62*, 1792–1811.
Branstator, G. (1987), A striking example of the atmosphere's leading traveling pattern, *J. Atmos. Sci.*, *44*, 2310–2323.
Branstator, G. (2014), Long-lived response of the mid-latitude circulation and storm tracks to pulses of tropical heating, *J. Clim.*, *27*, 8809–8826.
Branstator, G., and J. D. Opsteegh (1989), Free solutions of the barotropic vorticity equation, *J. Atmos. Sci.*, *46*, 1799–1814.
Branstator, G., and F. Selten (2009), "Modes of variability" and climate change, *J. Clim.*, *22*, 2639–2658.
Buizza, R., M. Miller, and T. N. Palmer (1999), Stochastic representation of model uncertainties in the ECMWF ensemble prediction system, *Q. J. R. Meteorol. Soc.*, *125*, 2887–2908.
Burrows, W. R., M. Benjamin, S. Beauchamp, E. R. Lord, D. McCollor, and D. Thomson (1995), CART decision-tree statistical analysis and prediction of summer season maximum surface ozone for Vancouver, Montreal and Atlantic regions of Canada, *J. Appl. Meteorol.*, *34*, 1848–1862.
Cash, B. A., and S. Lee (2001), Observed nonmodal growth of the Pacific-North American teleconnection pattern, *J. Clim.*, *14*, 1017–1028.
Casola, J. H., and J. M. Wallace (2007), Identifying weather regimes in the wintertime 500-hPa geopotential height field for the Pacific-North American sector using a limited contour clustering technique, *J. Appl. Meteorol. Climatol.*, *46*, 1619–1630.
Cassano, E. N., A. H. Lynch, J. J. Cassano, and M. R. Koslow (2006), Classification of synoptic patterns in the western Arctic associated with extreme events at Barrow, Alaska, USA, *Clim. Res.*, *30*, 83–97.
Cassou, C. (2008), Intra-seasonal interaction between the Madden-Julian Oscillation and the North Atlantic Oscillation, *Nature*, *455*, 523–527.
Cassou, C., L. Terray, J. W. Hurrell, and C. Deser (2004), North Atlantic winter climate regimes: Spatial asymmetry, stationarity with time and oceanic forcing, *J. Clim.*, *17*, 1055–1068.
Cassou, C., L. Terray, and A. S. Phillips (2005), Tropical Atlantic influence on European heat waves, *J. Clim.*, *18*, 2805–2811.
Cassou, C, M Minvielle, L Terray, and C. Périgaud (2011), A statistical-dynamical scheme for reconstructing ocean forcing in the Atlantic. Part I: Weather regimes as predictors for ocean surface variables, *Clim. Dyn.*, *36*, 19–39.
Casty, C., D. Handorf, C. C. Raible, J. F. González-Rouco, E. Xoplaki, J. Luterbacher, A. Weisheimer, K. Dethloff, and H. Wanner (2005), Recurrent climate winter regimes in reconstructed and modeled 500-hPa geopotential height fields over the North Atlantic/European sector 1659–1990, *Clim. Dyn.*, *24*, 809–822.
Cattiaux, J., B. Quesada, A. Arakelian, F. Codron, R. Vautard, and P. Yiou (2013), North-Atlantic dynamics and European temperature extremes in the IPSL model: Sensitivity to atmospheric resolution, *Clim. Dyn.*, *40*, 2293–2310.
Catto, J. L. (2016), Extratropical cyclone classification and its use in climate studies, *Rev. Geophys.*, *54*, 486–520, doi:10.1002/2016RG000519.
Cehelesky, P, and K. K. Tung (1987), Theories of multiple equilibria and weather regimes—A critical reexamination. Part II: Baroclinic two-layer models, *J. Atmos. Sci.*, *44*, 3282–3303.
Cerlini, P. B., S. Corti, and S. Tibaldi (1999), An intercomparison between low-frequency variability indices, *Tellus A*, *51*, 773–789.
Charney, J. G., and J. G. Devore (1979), Multiple flow equilibria in the atmosphere and blocking, *J. Atmos. Sci.*, *36*, 1205–1216.

Charney, J. G., and D. M. Straus (1980), Form-drag instability, multiple equilibria and propagating planetary waves in baroclinic, orographically forced, planetary wave systems, *J. Atmos. Sci.*, *37*, 1157–1176.
Charney, J. G., J. Shukla, and K. C. Mo (1981), Comparison of a barotropic blocking theory with observation, *J. Atmos. Sci.*, *38*, 762–799.
Cheng, X., and J. M. Wallace (1993), Cluster analysis of the Northern Hemisphere wintertime 500-hPa height field: Spatial patterns, *J. Atmos. Sci.*, *50*, 2674–2696.
Chessa, P. A., and F. Lalaurette (2001), Verification of the ECMWF ensemble prediction system forecasts: A study of large-scale patterns, *Weather Forecasting*, *16*, 611–619.
Christiansen, B. (2003), Evidence for nonlinear climate change: Two stratospheric regimes and a regime shift, *J. Clim.*, *16*, 3681–3690.
Christiansen, B. (2005), Bimodality of the planetary-scale atmospheric wave amplitude index, *J. Atmos. Sci.*, *62*, 2528–2541.
Christiansen, B. (2007), Atmospheric circulation regimes: Can cluster analysis provide the number?, *J. Clim.*, *20*, 2229–2250.
Christensen, H. M., I. M. Moroz, and T. N. Palmer (2015), Simulating weather regimes: Impact of stochastic and perturbed parameter schemes in a simple atmospheric model, *J. Clim.*, *44*, 2195–2214.
Coleman, J. S., and J. C. Rogers (2007), A synoptic climatology of the Central United States and associations with Pacific teleconnection pattern frequency, *J. Clim.*, *20*, 3485–2497.
Colucci, S. J., and D. P. Baumhefner (1992), Initial weather regimes as predictors of numerical 30-day mean forecast accuracy, *J. Atmos. Sci.*, *49*, 1652–1671.
Corti, S., F. Molteni, and T. N. Palmer (1999), Signature of recent climate change in frequencies of natural atmospheric circulation regimes, *Nature*, *398*, 799–802.
Corti, S., S. Gualdi, and A. Navarra (2003), Analysis of the mid-latitude weather regimes in the 200-year control integration of the SINTEX mode, *Ann. Geophys.*, *46*, 27–37.
Coumou, D., V. Petoukhov, S. Rahmstorf, S. Petri, and H. J. Schellnhuber (2014), Quasi-resonant circulation regimes and hemispheric synchronization of extreme weather in boreal summer, *Proc. Natl. Acad. Sci. U.S.A.*, *111*, 12331–12336.
Crommelin, D. T. (2003), Regime transitions and heteroclinic connections in a barotropic atmosphere, *J. Atmos. Sci.*, *60*, 229–246.
Crommelin, D. T. (2004), Observed non-diffusive dynamics in large-scale atmospheric flow, *J. Atmos. Sci.*, *61*, 2348–2396.
Dawson, A., and T. N. Palmer (2014), Simulating weather regimes: Impact of model resolution and stochastic parameterization, *Clim. Dyn.*, *44*, 2177–2193.
Dawson, A, T. N. Palmer, and S. Corti (2012), Simulating regime structures in weather and climate prediction models, *Geophys. Res. Lett.*, *39*, L21805, doi:10.1029/2012GL053284.
D'Andrea, F, and R. Vautard (2001), Extra tropical low-frequency variability as a low-dimensional problem. Part I: A simplified model, *Q. J. R. Meteorol. Soc.*, *127*, 1357–1374.
D'Andrea, F, and R. Vautard (2002), Extra tropical low-frequency variability as a low-dimensional problem. Part II: Stationarity and stability of large-scale equilibria, *Q. J. R. Meteorol. Soc.*, *128*, 1059–1074.
Davini, P., and C. Cagnazzo (2014), On the misinterpretation of the North Atlantic Oscillation in CMIP5 models, *Clim. Dyn.*, *43*, 1497–1511.
Deland, R. (1964), Traveling planetary waves, *Tellus*, *16*, 271–273.
Deloncle, A., R. Berk, R. D'Andrea, and M. Ghil (2007), Weather regime prediction using statistical learning, *J. Atmos. Sci.*, *64*, 1619–1635.
DelSole, T., and P. Chang (2003), Predictable component analysis, canonical correlation analysis, and autoregressive models, *J. Atmos. Sci.*, *60*, 409–416.
Delsole, T., and B. Farrell (1995), A stochastically excited linear system as a model for quasi-geostrophic turbulence: Analytic results for one- and two-layer fluids, *J. Atmos. Sci.*, *52*, 2531–2547.
Ding, Q., and B. Wang (2005), Circumglobal teleconnection in the Northern Hemisphere summer, *J. Clim.*, *18*, 3483–3505.
Dole, R. M. (1986), Persistent anomalies of the extra-tropical Northern Hemisphere wintertime circulation: Structure, *Mon. Weather Rev.*, *114*, 178–207.
Dole, R. M., and N. M. Gordon (1983), Persistent anomalies of the extra-tropical Northern Hemisphere wintertime circulation: Geographical distribution and regional persistence characteristics, *Mon. Weather Rev.*, *111*, 1567–1587.
Dommenget, D. (2007), Evaluating EOF modes against a stochastic null hypothesis, *Clim. Dyn.*, *28*, 517–531.
Driouech, F., M. Déqué, and E. Sánchez-Gómez (2010), Weather regimes—Moroccan precipitation link in a regional climate change simulation, *Global Clim. Change*, *72*, 1–10.
Enke, W., and A. Spekat (1997), Downscaling climate model outputs into local and regional weather elements by classification and regression, *Clim. Res.*, *8*, 195–207.
Farrara, J. D., M. Ghil, and C. R. Mechoso (1989), Empirical orthogonal functions and multiple flow regimes in the Southern Hemisphere winter, *J. Atmos. Sci.*, *46*, 3219–3223.
Farrell, B. F., and P. J. Ioannou (2000), Transient and asymptotic growth of two dimensional perturbations in viscous compressible shear flow, *Phys. Fluids*, *12*, 3021–3028.
Feldstein, S. B. (2000), The timescale, power spectra, and climate noise properties of teleconnection patterns, *J. Clim.*, *13*, 4430–4440.
Ferranti, L., and S. Corti (2011), New clustering products, *ECMWF Newslett.*, *127*, 6–11.
Ferranti, L, T. N. Palmer, F. Molteni, and E. Klinker (1990), Tropical-extratropical interaction associated with the 30–60 day oscillation and its impact on medium and extended range prediction, *J. Atmos. Sci.*, *47*, 2177–2199.
Ferranti, L., S. Corti, and M. Janousek (2015), Flow-dependent verification of the ECMWF ensemble over the Euro-Atlantic sector, *Q. J. R. Meteorol. Soc.*, *141*, 916–924.
Fereday, D. R., J. R. Knight, A. A. Scaife, C. K. Folland, and A. Philipp (2008), Cluster analysis of North Atlantic-European circulation types and links with Tropical Pacific sea surface temperatures, *J. Clim.*, *21*, 3687–3703.
Fraedrich, K. (1990), European grosswetter during the warm and cold extremes of the El Niño/Southern Oscillation, *Int. J. Climatol.*, *10*, 21–31.
Fraedrich, K., K. Muller, and R. Kuglin (1992), Northern Hemisphere circulation regimes during the extremes of El Niño/Southern Oscillation, *Tellus*, *44A*, 33–40.
Fraley, C., and A. E. Raftery (1998), How many clusters? Which clustering method? Answers via model-based cluster analysis, *Comput. J.*, *41*, 528–588.
Fraley, C., and A. E. Raftery (2003), Enhanced Software for model-based clustering, discriminant analysis, and density estimation: MCLUST, *J. Classific.*, *20*, 263–286.
Frame, T. H., M. H. Ambaum, S. L. Gray, and J. Methven (2011), Ensemble prediction of transitions of the North Atlantic eddy-driven jet, *Q. J. R. Meteorol. Soc.*, *137*, 1288–1297.
Franzke, C. (2009), Multi-scale analysis of teleconnection indices: Climate noise and nonlinear trend analysis, *Nonlin. Proc. Geophys.*, *16*, 65–76.

Franzke, C. (2013), Circulation regimes and extreme events in the North Atlantic, *Philos. Trans. R. Soc. A*, *371*, 20110471.
Franzke, C., and S. B. Feldstein (2005), The continuum and dynamics of Northern Hemisphere teleconnection patterns, *J. Atmos. Sci.*, *62*, 3250–3267.
Franzke, C., and A. J. Majda (2006), Low-order stochastic mode reduction for a prototype atmospheric GCM, *J. Atmos. Sci.*, *63*, 457–479.
Franzke, C., and T. Woollings (2011), On the persistence and predictability properties of North Atlantic climate variability, *J. Clim.*, *24*, 466–472.
Franzke, C., S. Lee, and S. B. Feldstein (2004), Is the North Atlantic Oscillation a breaking wave?, *J. Atmos. Sci.*, *61*, 145–160.
Franzke, C., A. J. Majda, and E. Vanden-Eijnden (2005), Low-order stochastic mode reduction for a realistic barotropic model climate, *J. Atmos. Sci.*, *62*, 1722–1745.
Franzke, C., A. J. Majda, and G. Branstator (2007), The origin of nonlinear signatures of planetary wave dynamics: Mean phase space tendencies and contributions from non-Gaussianity, *J. Atmos. Sci.*, *64*, 3987–4003.
Franzke, C., D. T. Crommelin, A. Fischer, and A. J. Majda (2008), A hidden Markov model perspective on regimes and metastability in atmospheric flows, *J. Clim.*, *21*, 1740–1757.
Franzke, C., I. Horenko, A. J. Majda, and R. Klein (2009), Systematic metastable atmospheric regime identification in a AGCM, *J. Atmos. Sci.*, *66*, 1997–2012.
Franzke, C., S. B. Feldstein, and S. Lee (2011a), Synoptic analysis of the Pacific-North American teleconnection pattern, *Q. J. R. Meterol. Soc.*, *137*, 329–346.
Franzke, C., T. Woollings, and O. Martius (2011b), Persistent circulation regimes and preferred regime transitions in the North Atlantic, *J. Atmos. Sci.*, *68*, 2809–2825.
Franzke, C., D. Monselesan, T. O'Kane, J. Risbey, and I. Horenko (2015a), Systematic attribution of secular southern hemispheric circulation trends with observational forcing data, *Nonlin. Proc. Geophys*, *22*, 513–525.
Franzke, C., T. O'Kane, J. Berner, P. Williams, and V. Lucarini (2015b), Stochastic climate theory and modelling, *WIREs Clim. Change*, *6*, 63–78.
Frederiksen, J. S. (1982), A unified three-dimensional instability theory of the onset of blocking and cyclo-genesis, *J. Atmos. Sci.*, *39*, 969–982.
Frederiksen, J. S., and P. J. Webster (1988), Alternative theories of atmospheric teleconnections and low-frequency fluctuations, *Rev. Geophys.*, *26*, 459–494.
Gaffney, S. J., A. W. Robertson, P. Smyth, S. J. Camargo, and M. Ghil (2007), Probabilistic clustering of extra-tropical cyclone using regression mixture models, *Clim. Dyn.*, *29*, 123–440.
Ghil, M., and A. W. Robertson (2002), "Waves" vs. "particles" in the atmosphere's phase space: A pathway to long-range forecasting?, *Proc. Natl. Acad. Sci.*, *99*, 2493–2500.
Goodess, C. M., and P. D. Jones (2002), Links between circulation and changes in the characteristics of Iberian rainfall, *Int. J. Climatol.*, *22*, 1593–1615.
Goubanova, K., L. Li, P. Yiou, and F. Codron (2010), Relation between large-scale circulation and European winter temperature: Does it hold under global warming?, *Int. J. Clim.*, *23*, 3752–3760.
Haines, K., and A. Hannachi (1995), Weather regimes in the Pacific from a GCM, *J. Atmos. Sci.*, *52*, 2444–2462.
Handorf, D., and K. Dethloff (2012), How well do state-of-the-art atmosphere-ocean general circulation models reproduce atmospheric teleconnection patterns?, *Tellus*, *64A*, doi:10.3402/tellusa.v64i0.19777.
Handorf, D., K. Dethloff, A. G. Marshall, and A Lynch (2009), Climate regime variability for past and present time-slices simulated by the Fast Ocean Atmosphere Model, *J. Clim.*, *22*, 58–70.
Hannachi, A. (1997a), Weather regimes in the Pacific from a GCM. Part II: Dynamics and stability, *J. Atmos. Sci.*, *54*, 1334–1348.
Hannachi, A. (1997b), Low-frequency variability in a GCM: Three-dimensional flow regimes and their dynamics, *J. Clim.*, *10*, 1357–1379.
Hannachi, A. (2007), Tropospheric planetary wave dynamics and mixture modeling: Two preferred regimes and a regime shift, *J. Atmos. Sci.*, *64*, 3521–3541.
Hannachi, A. (2010), On the origin of planetary-scale extra-tropical winter circulation regimes, *J. Atmos. Sci.*, *67*, 1382–1401.
Hannachi, A., and A. O'Neill (2001), Atmospheric multiple equilibria and non-Gaussian behavior in model simulations, *Q. J. R. Meteorol. Soc.*, *127*, 939–958.
Hannachi, A., and A. J. Turner (2008), Preferred structures in large-scale circulation and the effect of doubling greenhouse gas concentration in HadCM3, *Q. J. R. Meteorol. Soc.*, *134*, 469–480.
Hannachi, A., and A. J. Turner (2013), 20th century intra-seasonal Asian monsoon dynamics viewed from Isomap, *Nonlin. Processes Geophys.*, *30*, 725–741.
Hannachi, A., I. T. Jolliffe, and D. B. Stephenson (2007), Empirical orthogonal functions and related techniques in atmospheric science: A review, *Int. J. Climatol.*, *27*, 7–28.
Hannachi, A., D. Mitchell, L. Gray, and A. Charlton-Perez (2011), On the use of geometric moments to examine the continuum of sudden stratospheric warmings, *J. Atmos. Sci.*, *68*, 657–674.
Hannachi, A., T. Woollings, and K. Fraedrich (2012), The North Atlantic jet stream: A look at preferred positions, paths and transitions, *Q. J. R. Meteorol. Soc.*, *138*, 862–877.
Hannachi, A., E. A. Barnes, and T. Woollings (2013), Behaviour of the winter North Atlantic eddy-driven jet stream in the CMIP3 integrations, *Clim. Dyn.*, *41*, 995–1007.
Hansen, A. R. (1986), Observational characteristics of atmospheric planetary waves with bimodal amplitude distributions, *Adv. Geophys.*, *29*, 101–133.
Hansen, A. R., and A. Sutera (1986), On the probability density distribution of large-scale atmospheric wave amplitude, *J. Atmos. Sci.*, *43*, 3250–3265.
Hansen, A. R., and A. Sutera (1995), The probability density distribution of large-scale atmospheric wave amplitude revisited, *J. Atmos. Sci.*, *52*, 2463–2472.
Hansen, A. R., A. Sutera, and J. J. Tribbia (1991), The relation of multiple flow regimes to climate error in general circulation models: Southern Hemisphere winter, *J. Atmos. Sci.*, *48*, 1329–1335.
Haurwitz, B. (1940), The motion of atmospheric disturbances on a spherical Earth, *J. Mar. Res.*, *3*, 254–267.
Held, I. M. (1983), Stationary and quasi-stationary eddies in the extratropical troposphere: Theory, in *Large-Scale Dynamical Processes in the Atmosphere*, edited by B. Hoskins and R. P. Pearce, pp. 127–168, Academic Press, London.
Hewitson, B. C., and R. G. Crane (2002), Self-organizing maps: Applications to synoptic climatology, *Clim. Res.*, *22*, 13–26.
Hirooka, T., and I. Hirota (1985), Normal mode Rossby waves observed in the upper stratosphere. Part II: Second antisymmetric modes of zonal wavenumbers 1 and 2, *J. Atmos. Sci.*, *42*, 536–548.

Hoffman, F. M., W. W. Hargrove, DJ. Erickson, and R. J. Oglesby (2005), Using clustered climate regimes to analyze and compare predictions from fully coupled general circulation models, *Earth Interact.*, *9*, 1–27.
Horel, J. D (1985), Persistence of 500-mb height field during Northern Hemisphere winter, *Mon. Weather Rev.*, *113*, 2030–2042.
Horel, J. D., and J. M. Wallace (1981), Planetary-scale atmospheric phenomena associated with the Southern Oscillation, *Mon. Weather Rev.*, *109*, 813–829.
Horenko, I. (2010), On the identification of non-stationary factor models and their application to atmospheric data sets, *J. Atmos. Sci.*, *67*, 1559–1574.
Hoskins, B. J. (1983), Dynamical processes in the atmosphere and the use of models, *Q. J. R. Meteorol. Soc.*, *109*, 1–21.
Hoskins, B. J., and T. Ambrizzi (1993), Rossby wave propagation on a realistic longitudinally varying flow, *J. Atmos. Sci.*, *50*, 1661–1671.
Hoskins, B. J., and D. J. Karoly (1981), The steady linear response of a spherical atmosphere to thermal and orographic forcing, *J. Atmos. Sci.*, *38*, 1179–1196.
Hoskins, B. J., and A. J. Simmons (1975), A multi-layer spectral model and the semi-implicit method, *Q. J. R. Meteorol. Soc.*, *101*, 637–655.
Hoskins, B. J., A. J. Simmons, and D. G. Andrews (1977), Energy dispersion in a barotropic atmosphere, *Q. J. R. Meteorol. Soc.*, *103*, 553–556.
Holzer, M. (1996), Asymmetric geopotential height fluctuations from symmetric winds, *J. Atmos. Sci.*, *53*, 1361–1371.
Hsu, C. J., and F. Zwiers (2001), Climate change in recurrent regimes and modes of atmospheric variability, *J. Geophys. Res.*, *106*(D17), 20,145–20,160.
Huth, R., C. Beck, A. Philipp, M. Demuzere, Z. Ustrnul, M. Cahynová, J. Kyselý, and O. E. Tveito (2008), Classifications of atmospheric circulation patterns, recent advances and applications, *Ann. N. Y. Acad. Sci.*, *1146*, 105–152.
Itoh, H., and M. Kimoto (1996), Multiple attractors and chaotic itinerancy in a quasi-geostrophic model with realistic topography: Implications for weather regimes and low-frequency variability, *J. Atmos. Sci.*, *53*, 2217–2231.
Itoh, H., and M. Kimoto (1997), Chaotic itinerancy with preferred transition routes appearing in an atmospheric model, *Phys. D*, *109*, 274–292.
Itoh, H., and M. Kimoto (1999), Weather regimes, low-frequency oscillations, and principal patterns of variability: A perspective of extra-tropical low-frequency variability, *J. Atmos. Sci.*, *56*, 2684–2705.
Itoh, H., M. Kimoto, and H. Aoki (1999), Alternation between the single and double jet structures in the Southern Hemisphere troposphere. Part I: Chaotic wandering, *J. Meteo. Soc. Jpn.*, *77*, 399–412.
James, P. M. (2006), An assessment of European synoptic variability in Hadley Centre Global Environmental models based on an objective classification of weather regimes, *Clim. Dyn.*, *27*, 215–231.
Johnson, N. C., and S. B. Feldstein (2010), The continuum of North Pacific sea level pressure patterns: Intraseasonal, interannual, and interdecadal variability, *J. Clim.*, *23*, 851–857.
Jung, T., M. J. Miller, T. N. Palmer, P. Towers, N. Wedi, D. Achuthavarier, J. M. Adams, E. L. Altshuler, B. A. Cash, J. L. Kinter, L. Marx, and C. Stan (2012), High-resolution global climate simulations with the ECMWF model in Project Athena: Experimental design, model climate, and seasonal forecast skill, *J. Clim.*, *25*, 33155–3172.
Kageyama, M., F. D'Andrea, G. Rammstein, P. J. Valdes, and R. Vautard (1999), Weather regimes in past climate atmospheric general circulation model simulations, *Clim. Dyn.*, *15*, 773–793.
Kasahara, A. (1980), Effect of zonal flows on the free oscillations of a barotropic atmosphere, *J. Atmos. Sci.*, *37*, 917–929.
Keeley, S. P. E., R. T. Sutton, and L. C. Shaffrey (2009), Weather regimes in past climate atmospheric general circulation model simulations, *Geophys. Res. Lett.*, *36*, L22706, doi:10.1029/2009GL040367.
Kimoto, M., and M. Ghil (1993a), Multiple flow regimes in the Northern Hemisphere winter: Part I: Methodology and hemispheric regimes, *J. Atmos. Sci.*, *50*, 2625–2643.
Kimoto, M., and M. Ghil (1993b), Multiple flow regimes in the Northern Hemisphere winter: Part II: Sectorial regimes and preferred transitions, *J. Atmos. Sci.*, *50*, 2645–2673.
Kimoto, M., M. Mukougawa, and S. Yoden (1992), Medium-range forecast skill variation and blocking transition: A case study, *Mon. Weather Rev.*, *120*, 1616–1627.
Kohonen, T. (2001), *Self Organizing Maps*, Springer, New York.
Kondrashov, D., S Kravtsov, and M. Ghil (2011), Signatures of nonlinear dynamics in an idealized atmospheric model, *J. Atmos. Sci.*, *68*, 3–12.
Koo, S., A. W. Robertson, and M. Ghil (2002), Multiple regimes and low-frequency oscillations in the Southern Hemisphere's zonal-mean flow, *J. Geophys. Res.*, *107*, 4596, doi:10.1029/2001JD001353.
Kravtsov, S., A. W. Robertson, and M. Ghil (2005), Bimodal behavior in the zonal mean flow of a baroclinic beta-channel model, *J. Atmos. Sci.*, *62*, 1746–1769.
Kravtsov, S., A. W. Robertson, and M. Ghil (2006), Multiple regimes and low-frequency oscillations in the Northern Hemisphere's zonal-mean flow, *J. Atmos. Sci.*, *63*, 840–860.
Kushnir, Y. (1987), Retrograding winter time low-frequency disturbance over the North Pacific Ocean, *J. Atmos. Sci.*, *44*, 2727–2742.
Langland, R. H., and R. N. Maue (2012), Recent Northern Hemisphere mid-latitude medium-range deterministic forecast skill, *Tellus A*, *64*, 1–10.
Lau, W. K. M., D. E. Waliser, and P. E. Roundy (2012), Tropical-extratropical interaction, in *Intraseasonal Variability in the Atmosphere-Ocean Climate System*, pp. 497–512, Springer, Berlin.
Legras, B., and M. Ghil (1985), Persistent anomalies, blocking and variations in atmospheric predictability, *J. Atmos. Sci.*, *42*, 433–471.
Leith, C. E (1973), The standard error of time-average estimates of climatic means, *J. Appl. Meteorol.*, *12*, 1066–1068.
Lejenäs, H., and R. A. Madden (1992), Traveling planetary-scale waves and blocking, *Mon. Weather Rev.*, *120*, 2821–2830.
Lin, H., G. Brunet, and J. Derome (2009), An observed connection between the North Atlantic Oscillation and the Madden-Julian Oscillation, *J. Clim.*, *22*, 364–380.
Lindzen, R. S., D. M. Straus, and B. Katz (1984), An observational study of large-scale atmospheric Rossby waves during FGGE, *J. Atmos. Sci.*, *41*, 1320–1335.
Liu, H., E. Tosi, and S. Tibaldi (2006), On the relationship between northern hemispheric weather regimes in wintertime and spring precipitation over China, *Q. J. R. Meteorol. Soc.*, *120*, 185–194.
Lorenz, E. N. (1963), Deterministic non-periodic flow, *J. Atmos. Sci.*, *20*, 130–141.
Lorenz, E. N. (1996), Predictability—A problem partly solved, in *Proceedings of Seminar on Predictability*, vol. 1, pp. 1–18, ECMWF, Shinfield Park, Reading.
Lorenz, E. N. (1970), Climate change as a mathematical problem, *J. Appl. Meteorol.*, *9*, 325–329.
Lorenz, D. J., and D. L. Hartmann (2003), Eddy-zonal flow feedback in the Northern Hemisphere winter, *J. Clim.*, *16*, 1212–1227.
Lorreya, A., A. M. Fowlera, and J. Salinger (2007), Regional climate regime classification as a quantitative tool for interpreting multi-proxy paleoclimate data spatial patterns: A New Zealand case study, *Palaeogeogr. Palaeoclimatol. Palaeoecol.*, *253*, 407–433.

Madden, R. A (1978), Further evidence of traveling planetary waves, *J. Atmos. Sci.*, *35*, 1605–1618.
Madden, R. A (2007), Large-scale, free Rossby waves in the atmosphere—An update., *Tellus*, *59A*, 571–590.
Martius, O., C. Schwierz, and H. C. Davies (2007), Breaking waves at the tropopause in the wintertime Northern Hemisphere: Climatological analyses of the orientation and the theoretical LC1/2 classification, *J. Atmos. Sci.*, *64*, 2576–2592.
Majda, A. J., I. Timofeyev, and E. Vanden-Eijnden (1999), Models for stochastic climate prediction, *Proc. Natl. Acad. Sci.*, *96*, 14687–14691.
Majda, A. J., C. Franzke, A. Fischer, and D. T. Crommelin (2006), Distinct atmospheric regimes despite nearly Gaussian statistics—A paradigm model, *Proc. Natl. Acad. Sci.*, *103*, 8309–8314.
Majda, A. J., C. Franzke, and B. Khouider (2008), An applied mathematics perspective on stochastic modelling for climate, *Philos. Trans. R. Soc. A*, *366*, 2429–2455.
Majda, A. J., C. Franzke, and D. Crommelin (2009), Normal forms for reduced stochastic climate models, *Proc. Natl. Acad. Sci.*, *106*, 3649–3653.
Marshall, J. C., and F. Molteni (1993), Toward a dynamical understanding of planetary-scale flow regimes, *J. Atmos. Sci.*, *50*, 1792–1818.
Marshall, J. C., and D. K. W. So (1990), Thermal equilibrium of planetary waves, *J. Atmos. Sci.*, *47*, 963–978.
Masato, G., B. J. Hoskins, and T. J. Woollings (2008), Can the frequency of blocking be described by a red noise process?, *J. Atmos. Sci.*, *66*, 2143–2149.
Masato, G., T. J. Woollings, and B. J. Hoskins (2014), Structure and impact of atmospheric blocking over the Euro-Atlantic region in present-day and future simulations, *Geophys. Res. Lett.*, *41*, 1051–1058.
Matthews, A. J., B. J. Hoskins, and M. Masutani (2004), The global response to tropical heating in the Madden-Julian oscillation during the northern winter, *Q. J. R. Meteorol. Soc.*, *130*, 1991–2011.
McIntyre, M. E., and T. N. Palmer (1983), Breaking planetary waves in the stratosphere, *Nature*, *305*, 593–600.
McMurdie, L. A., and J. H. Casola (2009), Weather regimes and forecast errors in the Pacific Northwest, *Weather Forecasting*, *24*, 829–842.
Meehl, G. A., et al. (2007), *Climate Change 2007: The Physical Science Basis. Contribution of Working Group I to the Fourth Assessment Report of the Intergovernmental Panel on Climate Change*, edited by S. Solomon et al., pp. 747–845.
Metzner, P., L. Putzig, and I. Horenko (2012), Analysis of persistent non-stationary time series and applications, *Commun. Appl. Math. Comp. Sci.*, *7*, 175–229.
Michelangeli, P. A., R. Vautard, and B. Legras (1995), Weather regimes: Recurrence and quasi-stationarity, *J. Atmos. Sci.*, *52*, 1237–1256.
Minvielle, M., C. Cassou, R. Bourdallé-Badie, L. Terray, and J. Najac (2011), *Clim. Dyn.*, *36*, 401–417.
Mitchell, H. L., and J. Derome (1983), Blocking-like solutions of the potential vorticity equation: Their stability at equilibrium and growth at resonance, *J. Atmos. Sci.*, *40*, 2522–2536.
Mitchell, D., et al. (2016), Assessing mid-latitude dynamics in extreme event attribution systems, *Clim. Dyn.*, *40*, 1–13, doi:10.1007/s00382-016-3308-z.
Mo, K. C., and M. Ghil (1987), Statistics and dynamics of persistent anomalies, *J. Atmos. Sci.*, *44*, 877–901.
Mo, K. C., and M. Ghil (1988), Cluster analysis of multiple planetary flow regimes, *J. Geophys. Res.*, *93D*, 10,927–10,952.
Molteni, F., and S. Corti (1998), Long term fluctuations in the statistical properties of low-frequency variability: Dynamical origin and predictability, *Q. J. R. Meteorol. Soc.*, *124*, 495–526.
Molteni, F., and S. Tibaldi (1990), Regimes in the wintertime circulation over northern extra-tropics. II: Consequences for dynamical predictability, *Q. J. R. Meteorol. Soc.*, *116*, 1263–1288.
Molteni, F., M. O. King, F. Kucharski, and D. M. Straus (2011), Planetary-scale variability in the northern winter and the impact of land-sea thermal contrast, *Clim. Dyn.*, *37*, 151–170.
Monahan, A. H., and J. C. Fyfe (2006), On the nature of zonal jet EOFs, *J. Clim.*, *19*, 6409–6424.
Monahan, A. H., J. C. Fyfe, and G. M. Flato (2000), A regime view of Northern Hemisphere atmospheric variability and change under global warming, *Geophys. Res. Lett.*, *27*, 1139–1142.
Mori, M., and M. Watanabe (2008), The growth and triggering mechanisms of the PNA: A MJO-PNA coherence, *J. Meteorol. Soc. Jpn.*, *86*, 213–236.
Mukougawa, H. (1988), A dynamical model of "quasi-stationary" states in large scale atmospheric motions, *J. Atmos. Sci.*, *45*, 2868–2888.
Nakamura, H., and J. M. Wallace (1991), Skewness of low-frequency fluctuations in the tropospheric circulation during the Northern Hemisphere winter, *J. Atmos. Sci.*, *85*, 1441–1448.
Nakamura, H., M. Nakamura, and J. L. Anderson (1997), The role of high- and low frequency dynamics in blocking formation, *Mon. Weather Rev.*, *125*, 2074–2093.
Namias, J. (1950), The index cycle and its role in the general circulation, *J. Meteorol.*, *7*, 130–139.
Namias, J. (1964), Seasonal persistence and recurrence of European blocking during 1958–1960, *Tellus*, *16*, 94–407.
Newman, M., P. D. Sardeshmukh, and C. Penland (1997), Stochastic forcing of the wintertime extra-tropical flow, *J. Atmos. Sci.*, *54*, 435–455.
Newman, M., P. D. Sardeshmukh, C. R. Winkler, and J. S. Whitaker (2003), A study of sub-seasonal predictability, *Mon. Weather Rev.*, *131*, 1715–1732.
Newman, M., P. D. Sardeshmukh, and C. Penland (2009), How important is air-sea coupling in ENSO and MJO evolution?, *J. Clim.*, *22*, 2958–2977.
Nitsche, G., J. M. Wallace, and C. Kooperberg (1994), Is there evidence of multiple equilibria in planetary wave amplitude statistics?, *J. Atmos. Sci.*, *51*, 314–322.
Ortiz-Beviá, M. J., E. Sánchez Gómez, and F. J. Alvarez-Garcia (2011), North Atlantic atmospheric regimes and winter extremes in the Iberian Peninsula, *Nat. Hazards Earth Sys. Sci.*, *11*, 971–980.
O'Kane, T. J., J. S. Risbey, C. Franzke, I. Horenko, and D. P. Monselesan (2013), Changes in the meta-stability of the mid-latitude Southern Hemisphere circulation and the utility of non-stationary cluster analysis and split flow indices as diagnostic tools, *J. Atmos. Sci.*, *70*, 824–842.
Palmer, T. N. (1993), Extended-range atmospheric prediction and the Lorenz model, *Bull. Am. Meteorol. Soc.*, *74*, 49–65.
Palmer, T. N. (1999), A nonlinear dynamical perspective on climate prediction, *J. Clim.*, *12*, 575–591.
Pandolfo, l. (1993), Observational aspects of the low-frequency intra-seasonal variability of the atmosphere in middle latitudes, *Adv. Geophys.*, *34*, 93–174.
Peavoy, D., C. Franzke, and G. O. Roberts (2015), Physics constrained parameter estimation of stochastic differential equations, *Comp. Stat. Data Anal.*, *83*, 182–199.
Penland, C. (1989), Random forcing and forecasting using principal oscillation pattern analysis, *Mon. Weather Rev.*, *117*, 2165–2185.
Penland, C., and P. Sardeshmukh (1995), The optimal growth of tropical sea surface temperature anomalies, *J. Clim.*, *8*, 1999–2024.
Penland, C., M. Flugel, and P. Chang (2000), Identification of dynamical regimes in an intermediate coupled ocean-atmosphere model, *J. Clim.*, *13*, 2105–2115.
Perron, M., and P. Sura (2013), Climatology of non-Gaussian atmospheric statistics, *J. Clim.*, *26*, 1063–1083.

Petoukhov, V., S. Rahmstorf, S. Petri, and H. J. Schellnhuber (2013), Quasi-resonant amplification of planetary waves and recent Northern Hemisphere weather extremes, *Proc. Natl. Acad. Sci.*, *110*, 5336–5341.
Plaut, G., and E. Simonnet (2001), Large-scale circulation classification, weather regimes, and local climate over France, the Alps and Western Europe, *Clim. Res.*, *17*, 303–324.
Polo, I., A. Ullmann, P. Roucou, and B. Fontaine (2011), Weather regimes in the Euro-Atlantic and Mediterranean sector and relationship with West African rainfall over the period 1989–2008 from a self-organizing maps approach, *J. Clim.*, *24*, 3423–3432.
Polo, I., A. Ullmann, B. Fontaine, T. Losada, and P. Roucou (2013), Changes in the frequency of weather regimes over the Euro-Atlantic and Mediterranean sector and their relation to the anomalous temperatures over the Mediterranean sea, *Fisica de la Tierra*, *25*, 103–121.
Ponater, M., W. Konig, R. Sausen, and F. Sielmann (1994), Circulation regime fluctuations and their effect on intra-seasonal variability in the ECHAM climate model, *Tellus*, *46A*, 265–285.
Quadrelli, R., and J. M. Wallace (2004), A simplified linear framework for interpreting patterns of Northern Hemisphere wintertime climate variability, *Int. J. Clim.*, *17*, 3728–3744.
Quiroz, R. (1987), Traveling waves and regional transitions in blocking activity in the Northern Hemisphere, *Mon. Weather Rev.*, *115*, 919–935.
Rabiner, L. R. (1989), A tutorial on hidden Markov models and selected applications in speech recognition, *Proc. IEEE*, *177*, 257–286.
Raible, C. C., U. Luksch, K. Fraedrich, and R. Voss (2001), North Atlantic decadal regimes in a coupled GCM simulation, *Clim. Dyn.*, *18*, 321–330.
Reinhold, B. B., and R. T. Pierrehumbert (1982), Dynamics of weather regimes: Quasi-stationary waves and blocking, *Mon. Weather Rev.*, *110*, 1105–1145.
Reusch, D. B., R. B. Alley, and B. C. Hewitson (2007), North Atlantic climate variability from a self-organizing map perspective, *J. Geophys. Res.*, *112*, D02104, doi:10.1029/2006JD007460.
Rex, D. (1950a), Blocking action in the middle troposphere and its effect upon regional climate. I. An aerological study of blocking action, *Tellus*, *2*, 196–211.
Rex, D. (1950b), Blocking action in the middle troposphere and its effect upon regional climate. The climatology of blocking action, *Tellus*, *2*, 275–301.
Rex, D. (1961), The effect of Atlantic blocking upon European climate, *Tellus*, *3*, 1–16.
Risbey, J., T. O'Kane, D. Monselesan, C. Franzke, and I. Horenko (2015), Metastability of Northern Hemisphere teleconnection modes, *J. Atmos. Sci.*, *72*, 35–54.
Rivière, G., and I. Orlanski (2007), Characteristics of the Atlantic storm-track eddy activity and its relation with the North Atlantic Oscillation, *J. Atmos. Sci.*, *64*, 241–266.
Robertson, A. W., and M. Ghil (1999), Large-scale weather regimes and local climate over the western United States, *J. Clim.*, *12*, 1796–1813.
Robertson, A. W., and C. R. Mechoso (2003), Circulation regimes and low-frequency oscillations in the south Pacific sector, *Mon. Weather Rev.*, *131*, 1566–1576.
Robertson, A. W., M. Ghil, and M. Latif (2000), Inter-decadal changes in atmospheric low-frequency variability with and without boundary forcing, *J. Atmos. Sci.*, *57*, 1132–1140.
Robertson, A. W., Y. Kushnir, U. Lall, and J. Nakamura (2015), Weather and climatic drivers of extreme flooding events over the midwest of the United States, in *Extreme Events: Observations, Modeling, and Economics*, edited by M. Chavez, M. Ghil, and J. Urrutia-Fucugauchi, pp. 115–124, John Wiley, Hoboken, N. J., doi:10.1002/9781119157052.ch9.
Rojas, M., L. Z. Li, M. Kanakidou, N. Hatzianastassiou, G. Seze, and H. Le Treut (2013), Winter weather regimes over the Mediterranean region: Their role for the regional climate and projected changes in the twenty-first century, *Clim. Dyn.*, *41*, 551–571.
Roller, C. D., J.-H. Oian, L. Agel. M. Barlow, and V. Moron (2016), Winter weather regimes in the northeast United States, *J. Clim.*, *29*, 2963–2980.
Rossby, C.-G., et al. (1939), Relation between variations in the intensity of the zonal circulation of the atmosphere and the displacement of the semi-permanent centers of action, *J. Mar. Res.*, *2*, 39–54.
Rossby, C.-G., et al. (1940), Planetary flow patterns in the atmosphere, *Q. J. R. Meteorol. Soc.*, *66*, 68–87.
Ruti, P. M., V. Lucarini, A. D. Aquila, S. Calmanti, and A. Speranza (2006), Does the subtropical jet catalyze the mid-latitude atmospheric regimes?, *Geophys. Res. Lett.*, *33*, L06814, doi:10.1029/2005GL024620.
Salby, M. L. (1984), Survey of planetary-scale traveling waves: The theory and observations, *Rev. Geophys.*, *209*, 209–236.
Sardeshmukh, P. D., and B. J. Hoskins (1985), Vorticity balances in the tropics during the 1982–83 El Niño–Southern Oscillation event, *Q. J. R. Meteorol. Soc.*, *11*, 261–278.
Sardeshmukh, P. D., and P. Sura (2009), Reconciling non-Gaussian climate statistics with linear dynamics, *J. Clim.*, *22*, 1193–1207.
Schuenemann, K. C., and J. J. Cassano (2010), Changes in synoptic weather patterns and Greenland precipitation in the 20th and 21st centuries: 2. Analysis of 21st century atmospheric changes using self-organizing maps, *J. Geophys. Res.*, *115*, D05108, doi:10.1029/2009JD011706.
Sempf, M., K. Dethloff, D. Handorf, and M. Kurgansky (2007a), Circulation regimes due to attractor merging in atmospheric models, *J. Atmos. Sci.*, *64*, 2029–2044.
Sempf, M., K. Dethloff, D. Handorf, and M. Kurgansky (2007b), Towards understanding the dynamical origin of atmospheric regime behavior in a baroclinic model, *J. Atmos. Sci.*, *64*, 887–904.
Seo, K.-H., and S.-W. Son (2012), The global atmospheric circulation response to tropical diabatic heating associated with the Madden-Julian Oscillation during northern winter, *J. Atmos. Sci.*, *69*, 79–96.
Simonnet, E., and G. Plaut (2001), Space-time analysis of geopotential height and SLP, intra-seasonal oscillations, weather regimes, and local climates over the North Atlantic and Europe, *Clim. Res.*, *17*, 325–342.
Selten, F. M., and G. Branstator (2004), Preferred regime transition routes and evidence for an unstable periodic orbit in a baroclinic model, *J. Atmos. Sci.*, *61*, 2267–2282.
Shutts, G. J. (1987), Some comments on the concept of thermal forcing, *Q. J. R. Meteorol. Soc.*, *113*, 1387–1394.
Silverman, B. W. (1986), *Density Estimation for Statistics and Data Analysis*, Chapman and Hall, New York.
Simmons, A. J., J. M. Wallace, and G. W. Branstator (1983), Barotropic wave propagation and instability, and atmospheric teleconnection patterns, *J. Atmos. Sci.*, *40*, 1363–1392.
Smyth, P., M. Ghil, and K. Ide (1999), Multiple regimes in Northern Hemisphere height fields via mixture model clustering, *J. Atmos. Sci.*, *56*, 3704–3723.
Solman, S. A., and C. G. Mendez (2003), Weather regimes in the South American sector and neighboring oceans during winter, *Clim. Dyn.*, *21*, 91–104.

Solman, S. A., and H. Le Treut (2006), Climate change in terms of modes of atmospheric variability and circulation regimes over southern South America, *Clim. Dyn.*, *26*, 835–854. 34, 337–342.
Stan, D., and D. M. Straus (2007), Is blocking a circulation regime?, *Mon. Weather Rev.*, *135*, 2406–2413.
Stephenson, D. B., A. Hannachi, and A. O'Neill (2004), On the existence of multiple climate regimes, *Q. J. R. Meteorol. Soc.*, *130*, 583–605.
Straus, D. M. (2010), Synoptic-eddy feedbacks and circulation regime analysis, *Mon. Weather Rev.*, *138*, 4026–4034.
Straus, D. M., and J. Shukla (2002), Does ENSO force the PNA?, *J. Clim.*, *15*, 2340–2358.
Straus, D. M., and F. Molteni (2004), Flow regimes, SST forcing, and climate noise: Results from large GCM ensembles, *J. Clim.*, *17*, 1641–1656.
Straus, D. M., S. Corti, and F. Molteni (2007), Circulation regimes: Chaotic variability versus SST-forced predictability, *J. Clim.*, *20*, 2251–2272.
Straus, D. M., E. Swenson, and C.-L. Lappen (2015), The MJO cycle forcing of the North Atlantic circulation: Intervention experiments with the Community Earth System Model, *J. Atmos. Sci.*, *72*, 660–681.
Straus, D. M., F. Molteni, and S. Corti (2017), Atmospheric regimes: The link between weather and the large scale circulation, in *Nonlinear and Stochastic Climate Dynamics*, edited by C. L. E. Franzke and T. J. O'Kane, pp. 105–135, Cambridge Univ. Press, Cambridge, U. K.
Sura, P. (2011), A general perspective of extreme events in weather and climate, *Atmos. Res.*, *101*, 1–21.
Sura, P. (2013), Stochastic models of climate extremes: Theory and observations, in *Extremes in a Changing Climate*, edited by A. AghaKouchak et al., pp. 181–222, Springer, Dordrecht, Netherlands.
Sura, P., and A. Hannachi (2015), Perspectives of non-Gaussianity in atmospheric synoptic and low-frequency variability, *J. Clim.*, *28*, 5091–5114.
Sura, P., M. Newman, C. Penland, and P. Sardeshmukh (2005), Multiplicative noise and non-Gaussianity: A paradigm for atmospheric regimes?, *J. Atmos. Sci.*, *62*, 1391–1409.
Sutera, A. (1980), On stochastic perturbations and large term climatic behavior, *Q. J. R. Meteorol. Soc.*, *107*, 137–151.
Sutera, A. (1986), Probability density distribution of large-scale atmospheric flow, *Adv. Geophys.*, *29*, 227–249.
Swanson, K. L. (2001), Upper-tropospheric potential vorticity fluctuations and the dynamical relevance of the time mean, *J. Atmos. Sci.*, *58*, 1815–1826.
Teng, A., J. C. Fyfe, and A. H. Monahan (2007), Northern Hemisphere circulation regimes, *Clim. Dyn.*, *28*, 867–879.
Terray, L., and C. Cassou (2002), Tropical Atlantic sea surface temperature forcing of quasi-decadal climate variability over the North Atlantic–European region, *J. Clim.*, *15*, 3170–3187.
Thompson, D., J. M. Wallace, and G. C. Hegerl (2000), Annular modes in the extratropical circulation. Part II: Trends, *J. Clim.*, *15*, 1018–1036.
Thompson, D., M. P. Baldwin, and J. M. Wallace (2002), Stratospheric connection to Northern Hemisphere wintertime weather: Implications for prediction, *J. Clim.*, *13*, 1421–1428.
Tibshirani, R., G. Walther, and T. Hastie (2001), Estimating the number of clusters in a data set via the gap statistic, *J. R. Stat. Soc.*, *163B*, 411–423.
Toth, Z. (1991), Circulation patterns in phase space: A multi-normal distribution?, *Mon. Weather Rev.*, *119*, 1501–1511.
Toth, Z. (1992), Quasi-stationary and transient periods in the Northern Hemisphere circulation series, *J. Clim.*, *5*, 1235–1247.
Toth, Z. (1993), Preferred and unpreferred circulations types in the Northern Hemisphere wintertime phase space, *J. Atmos. Sci.*, *50*, 2868–2888.
Trenberth, K. E., and K. C. Mo (1985), Blocking in the Southern Hemisphere, *Mon. Weather Rev.*, *113*, 3–21.
Tryhom, L., and A. Degaetano (2011), A comparison of techniques for downscaling extreme precipitation over the northeastern United States, *Int. J. Climatol.*, *31*, 1975–1989.
Tung, K. K., and A. J. Rosenthal (1985), Theories of multiple equilibria—A critical reexamination. Part I: Barotropic models, *J. Atmos. Sci.*, *42*, 2804–2819.
Tung, K. K., and A. J. Rosenthal (1986), On the extended-range predictability of large scale quasi-stationary patterns in the atmosphere, *Tellus*, *38A*, 333–365.
Ullmann, A., B. Fontaine, and P. Roucou (2014), Euro-Atlantic weather regimes and Mediterranean rainfall patterns: Present-day variability and expected changes under CMIP5 projections, *Int. J. Climatol.*, *34*, 2634–2650.
Vallis, G. K., and E. P. Gerber (2008), Local and hemispheric dynamics of the North Atlantic Oscillation, annular patterns and the zonal index, *Dyn. Atmos. Oceans*, *44*, 184–221.
van den Besselaar, E. J. M., A. M. G. Klein Tank, and G. van der Schrier (2010), Influence of circulation types on temperature extremes in Europe, *Theor. Appl. Climatol.*, *99*, 431–439.
Vannitsem, S. (2001), Toward a phase-space cartography of the short- and medium-range predictability of weather regimes, *Tellus*, *53A*, 56–73.
Vautard, R. (1990), Multiple weather regimes over the North Atlantic: Analysis of precursors and successors, *Mon. Weather Rev.*, *118*, 2056–2081.
Vautard, R., and B. Legras (1988), On the source of low-frequency variability. Part II: Nonlinear equilibration of weather regimes, *J. Atmos. Sci.*, *45*, 2845–2867.
Vitart, F., and F. Molteni (2010), Simulation of the Madden-Julian-Oscillation and its teleconnections in the ECMWF forecast system, *Q. J. R. Meteorol. Soc.*, *136*, 842–855.
Vrac, M., M. Stein, and K. Hayhoe (2007), Statistical downscaling of precipitation through non-homogeneous stochastic weather typing, *Clim. Res.*, *34*, 169–184.
Wallace, J. M., and D. S. Gutzler (1981), Teleconnections in the geopotential height field during the Northern Hemisphere winter, *Mon. Weather Rev.*, *109*, 784–812.
Wallace, J. M., X. Cheng, and D. Sun (1991), Does low-frequency atmospheric variability exhibit regime-like behavior?, *Tellus*, *43*, 16–26.
Weisheimer, A, D. Handorf, and K. Dethloff (2001), On the structure and variability of atmospheric general circulation regime in coupled climate models, *Atmos. Sci. Lett.*, *2*, 72–80, doi:10.1006/asle.2001.0034.
Weisheimer, A., S. Corti, T. N. Palmer, and F. Vitart (2014), Addressing model error through atmospheric stochastic physical parametrizations: Impact on the coupled ECMWF seasonal forecasting system, *Philos. Trans. R. Soc. A*, *372*, 20130290, doi:10.1098/rsta.2013.0290.
Whitaker, J. S., and P. D. Sardeshmukh (1988), A linear theory of extra-tropical synoptic eddy statistics, *J. Atmos. Sci.*, *55*, 237–258.
White, G. H. (1980), Skewness, kurtosis and extreme values of Northern Hemisphere geopotential height, *Mon. Weather Rev.*, *108*, 1446–1455.
Wiin-Nielsen, A. (1979), Steady states and stability properties of a low order barotropic system with forcing and dissipation, *Tellus*, *31*, 375–386.
Williams, K. D., et al. (2015), The Met Office Global Coupled model 2.0 (GC2) configuration, *Geosci. Model Dev.*, *8*, 1509–1524, doi:10.5194/gmd-8-1509-2015.

Winkler, C. R., M. Newman, and P. D. Sardeshmukh (2001), A linear model of wintertime low-frequency variability. Part I: Formulation and forecast skill, *J. Clim.*, *14*, 4474–4494.
Woollings, T. (2008), Vertical structure of anthropogenic zonal-mean atmospheric circulation change, *Geophys. Res. Lett.*, *35*, L19702, doi:10.1029/2008GL034883.
Woollings, T., A. Hannachi, B. J. Hoskins, and A. Turner (2010a), A regime view of the North Atlantic Oscillation and its response to anthropogenic forcing, *J. Clim.*, *23*, 1291–1307.
Woollings, T., A. Hannachi, and B. J. Hoskins (2010b), Variability of the North Atlantic eddy-driven jet stream, *Q. J. R. Meteorol. Soc.*, *136*, 856–868.
Woollings, T. J., B. J. Hoskins, M. Blackburn, and P. Berrisford (2008), A new Rossby wave-breaking interpretation of the North Atlantic Oscillation, *J. Atmos. Sci.*, *65*, 609–626.
Yang, S., and B. Reinhold (1991), How does the low-frequency variance vary?, *Mon. Weather Rev.*, *119*, 119–127.
Yang, S., B. Reinhold, and E. Kallen (1997), Multiple weather regimes and baroclinically forced spherical resonance, *J. Atmos. Sci.*, *54*, 1397–1409.
Yiou, P., and M. Nogaj (2004), Extreme climate events and weather regimes over the North Atlantic: When and where?, *Geophys. Res. Lett.*, *31*, L07202, doi:10.1029/2003GL019119.
Yiou, P., K. Goubanova, Z. X. Li, and M. Nogaj (2008), Weather regime dependence of extreme value statistics for summer temperature and precipitation, *Nonlin. Processes Geophys.*, *15*, 365–378.
Yoden, S., M. Shiotani, and I. Hirota (1987), Multiple planetary flow regions in the Southern Hemisphere, *J. Meteorol. Soc. Japan*, *64*, 571–586.
Yuan, J., S. B. Feldstein, S. Lee, and B. Tan (2011), The relationship between the North Atlantic jet and tropical convection over the Indian and western Pacific Oceans, *J. Clim.*, *24*, 6100–6113.
Zhang, C. (2013), Madden-Julian Oscillation: Bridging weather and climate, *Bull. Am. Meteorol. Soc.*, *94*, 1849–1870.
Zhang, Y., J. M. Wallace, and N. Iwasaka (2005), Is climate variability over the North Pacific a linear response to ENSO?, *J. Clim.*, *9*, 1468–1478.
Zhengyu, L., and M. Alexander (2007), Atmospheric bridge, oceanic tunnel, and global climatic teleconnections, *Rev. Geophys.*, *45*, RG2005, doi:10.1029/2005RG000172.
Zorita, E., and H. von Storch (1999), The analog method as a simple statistical downscaling technique: Comparison with more complicated methods, *J. Clim.*, *12*, 2474–2489.